國立交通大學

電信工程學系

碩士論文

無線感測網路之線性最小平方差定位研究

Study on Linear Least-Squares Localization in Sensor Networks

研究生：徐泓聖

指導教授：謝世福　教授

中華民國九十八　年　六　月

無線感測網路之線性最小平方差定位研究

Study on Linear Least-Squares Localization in Sensor Networks

研 究 生：徐泓聖　　Student：H.S. Hsu

指導教授：謝世福　　Advisor：S. F. Hsieh

國 立 交 通 大 學

電信工程學系

碩 士 論 文

A Thesis

Submitted to Department of Communication Engineering

College of Electrical Engineering and Computer Science

National Chiao Tung University

In Partial Fulfillment of the Requirements

For the Degree of

Master of Science

In

Communication Engineering

June 2009

Hsinchu, Taiwan, Republic of China

中華民國九十八年六月

無線感測網路之線性最小平方差定位研究

學生:徐泓聖　　指導教授:謝世福

國立交通大學電信工程研究所

中文摘要

在室內及室外環境之下，估測出目標物(人或物)的位置有許多重要的應用。而 GPS 系統在被遮蔽的環境之下精準度不良，所以我們需要一個無線感測的定位系統。靠著許多感測器對於目標的距離(或角度)量測，透過定位之演算法，我們可以估算出待測物的位置。而感測器測距的準度越好，定位的準確度當然越好，所以我們修正傳統的相關測距法，利用訊號飛行時間和其能量的聯合關係，將可以提升精準度。另外，在測距時，感測器與待測物的直接路徑若不存在時，將會使得測到的距離過長，使位置估測產生很大的偏差。我們根據最大概似法，提出了減少誤差的方法。由於一般定位演算法是利用最小平方差方法來達成，其方程式為非線性方程式。為了降低運算複雜度，我們將探討三種典型的線性化方法，並分析其中兩種較常見線性化最小平方差方法之準確度。當感測器增加時，我們推導出準確度與感測器個數的關係。另外，當待測物移動時，其運動軌跡的估測也是定位技術中重要的議題。但過去利用 Kalman filter 來估測軌跡的運算複雜度過高，我們將其化簡，在準確度相差不大的結果下，進一步降低運算複雜度。

Study on Linear Least-Squares Localization in Sensor Networks

Student: H. S. Hsu **Advisor**：S. F. Hsieh

Department of Communication Engineering

National Chiao Tung University

Abstract

Sensor network localization relies on the range (or angle) measurement from the mobile (object) and the sensors with known positions. The location of the mobile can be estimated via these measurements. Accuracy of the localization algorithms highly depends on the accuracy of measured ranges. By considering both time-of-arrival (TOA) and received signal power, a range estimation method is proposed to improve ranging accuracy. Besides, the range measurement often suffers from non-line-of-sight (NLOS) effect and the range estimation might be much longer than the true range. As a result, the localization performance can degrade severely. We propose a NLOS mitigation algorithm based on simplified maximum-likelihood (ML). To alleviate the nonlinearity issue encountered in a least-squares localization model, three linearization techniques will be studied. Theoretical derivation shows that the asymptotic error is inversely proportional to the number of sensors. Besides, a simplified Kalman filter with lower complexity is proposed to track a moving mobile. Computer simulations will be performed to validate the theoretical analysis and compare performance of different algorithms.

Acknowledgment

轉眼間，在碩士班兩年的時間已過去，代表著我們將離開學校，面對未來工作及生活的各種挑戰。在這段做研究的期間，非常感謝指導教授謝世福老師的諄諄教悔，讓我在追求知識的過程中能以更嚴謹的思考方式進行，也在我遭遇瓶頸時給予適當的提點。另外，我也要感謝家人朋友們及以實驗室的大家，在我茫然失落時給我適時的鼓勵，讓我能夠順利的完成這兩年的學業。

Contents

List of Figures

List of Tables

Chapter 1
Introduction

There are more and more applications of sensor network localization [1-2,5,14] in recent years. For example, a self-cleaning robot must be localized and controlled. In healthcare applications, doctors and nurses need to know where the patients are to ensure their safety. In public occasions like museum, the location of visitors must be known to avoid them being lost.

Figure 1.1 shows a typical sensor network localization system. There are *N*

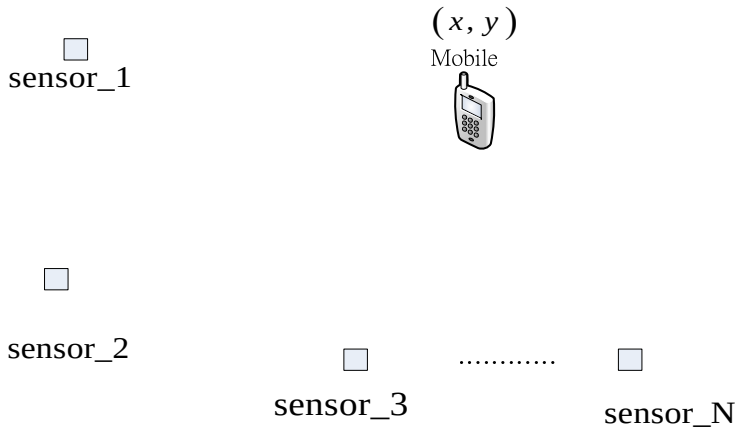

Figure 1.1 A typical sensor network localization system

distributed sensors and a mobile. The problem is how to estimate the position of the mobile via the information interaction between the unknown mobile and these distributed sensors with known positions. In case the positions of these sensors are also unknown to us, the localization problem would be more challenging [3].

Most common techniques for localizing a mobile use measurements of time-of-arrival (TOA) [4-5], time-difference-of-arrival (TDOA) [6-7], angle-of-arrival (AOA) [8-9], and received signal strength (RSS) [10-11]. Once we choose one kind , or a mixture [12], of these measured techniques, the position of mobile can be estimated by localization algorithms [13-14].

The localization accuracy highly depends on the accuracy of measurements. Correlator [43-44] is a typical method to estimate TOA. But this method is a suboptimal scheme, because it neglects the effect of signal power. Thus, we will propose a hybrid TOA and RSS scheme to improve the accuracy of TOA estimation.

The accuracy analysis [15-17] for location estimation is a crucial issue. [16] focused on the coverage issue and proposed two methods to estimate the lower bound of sensor density to guarantee a bounded localization error over the sensing field. [17] analyzed the localization accuracy of a linear least-squares (LS) technique theoretically. [17] also derived a closed-form mean square error (MSE) of the linear LS solution proposed in [18]. Based on [17], we will derive the asymptotic MSE theoretically when the number of sensors is large. In the other hand, we will also analyze the coverage issue in general localization scenario.

Generally, the measurements may suffer from multipath [19-21] effect. In UWB [22-23] systems, the mitigation for multipath has been widely discussed. [24] proposed a geometrically motivated approach that utilizes additional information from the auto-correlation of sensor signals and a zero TDOA sum condition to suppress spurious TDOA estimates. Another source localization approach by virtual sensors in a reverberant environment was also proposed in [25]. However, the problem of solving multipath error is not our concern in this thesis.

Besides, the measurements may also suffer from non-line-of-sight (NLOS) [26-29] effect. [26] proposed a NLOS identification technique based on the multipath

channel statistics. An effective technique is proposed in [27] for locating a mobile‘s position in NLOS environment by linearizing the inequalities of range models and adding loose variables. By modeling the TOA estimation error as Cauchy-Lorentz distribution, a robust source localization algorithm was derived in [30] to guard against outliers (include NLOS error). [29] proposed an optimal position estimation and a simple NLOS mitigation algorithm under NLOS environment. Based on [29], we extend to another NLOS bias estimation. Because the high complexity of the ML solution, we will propose a simplified ML estimation to mitigate NLOS effect.

In addition to solving the effect of multipath and NLOS, the tracking [31-33] of a moving mobile is another important issue in sensor network localization. While the mobile is moving, the main concern is to estimate its trajectory. Kalman filter[34-35] has been widely applied in trajectory estimation of a moving object. While its accuracy of tracking may be good enough , it needs a high computational cost. In this thesis, we adapt and simplify the update of Kalman filter, and proposed an adaptive localization scheme with lower complexity.

This thesis is organized as follows. We introduce localization techniques in Chapter 2 and proposed a hybrid ranging method based on TOA and RSS, then we focus on the theoretical error analysis for linear LS solutions in Chapter 3. The asymptotic mean-square-error will be derived in case of a large size of sensors. In Chapter 4, we first focus on the analysis of coverage issue. Next, we propose a simplified ML solution to mitigate NLOS effect. We will also propose an adaptive localization using simplified Kalman filter with low computational cost. Computer simulations of the derived analysis and proposed algorithms will be performed in Chapter 5. Finally, we give a conclusion of our work in Chapter 6.

Chapter 2
Localization Techniques

As mention in Chapter 1, the location estimation can be done via the measurements between the sensors and mobile. Four basic types of measurement techniques are introduced in Section 2.1. TOA estimation and a proposed hybrid scheme of TOA and RSS are discussed in Section 2.2.With the sensors at known positions and once the measurement information is obtained, the position of mobile can be estimated via localization algorithms. The localization algorithms are introduced in Sections 2.3-2.5.

2.1 Types of Measurements

Location sensing approaches typically use some characteristics of communication signal between sensors and mobile to estimate the location of mobile. Typically, the location of sensors must be known. According to the information of sensors, the mobile can obtain its location by the measurement of communication signal. In the following, we will discuss four major measurement techniques:

1. Angle of arrival (AOA)[8-9]: Angle of arrival is commonly used in direction-based systems. When the sensors receive signals from the mobile, the sensors can estimate the angle of the arrived signal. This approach requires the installation of a complex antenna array. All of AOA methods still need to concern the multi-path effect [19-21]. AOA is inapplicable for indoor environment or high node density network.

2. Received signal strength (RSS)[10-11]: There are many researches that focus on radio propagation models [36] by which we can calculate the distance from sensors to mobile. Cheap equipment with low computational cost is the main advantage of RSS-based localization method. But in the literature, it has been shown that RSS is not accurate enough, because there are many factors that can affect the RSS measurement [11]. For instance, multi-path, noise, humidity, temperature and so on.

3. Time of arrival (TOA)[4-5]: With an accurate time synchronization between sensors and mobile [38], the signal propagation time from mobile to sensor, or vice-versa, can be measured. Thus, the distance between sensor and mobile can be calculated by multiplying the propagation time with the signal propagation speed ($3\times10^{8} m/s$ for RF signal, or $\approx 340 m/s$ for acoustic signal). For indoor applications, high localization accuracy is required. The localization accuracy is highly dependent on the accuracy of measured ranging information. Compared to other measurement techniques, TOA techniques is a good candidate in terms of accuracy.

4. Time different of arrival (TDOA)[6-7]: TOA measurement relies on a precise time synchronization because the time when a signal leaves the emitter is generally not known. With the cross-correlation of two different sensors, the unknown time can be differentiated. Thus, the time difference of arrival between the two sensors can be measured. The main advantage of TDOA is the synchronization equipment is not necessary to install, but the accuracy of using the cross-correlation of two different sensors (both with noise) may degrade TDOA performance.

Owing to the reasons mentioned above, we focus on TOA measurement

technique in terms of accuracy and cost. With the TOA ranging data discussed in Section 2.2, the location can be estimated by the localization algorithms in Sections 2.4 and 2.5

2.2 TOA Ranging Technique

In this section, we discuss the range estimation by TOA technique. In Section 2.2.1 , we introduce conventional correlator–based TOA estimation. A hybrid scheme of TOA and RSS is proposed and discussed in Section 2.2.2.

2.2.1 Conventional Correlator-based TOA Estimation

First, the mobile transmits a signal *s(t)* to the sensors. The received signal at one sensor without multipath can be denoted as follows:

$$r(t) = \alpha s(t-\tau) + n(t) \qquad (2.1)$$

where $s(t)$ is the transmitted signal, which is usually a wideband signal, such as a PN signal or a chirp signal [44]. The issues of PN signal or chirp signal will be discussed in Section 5.1. τ is the time-of arrival of direct path, α is the gain of direct path, and $n(t)$ is the background noise.

We assume a synchronization equipment has been set up, and the sensor knows when the signal is transmitted. In other words, when the signal was transmitted from the mobile, the sensor started to receive. Optimum maximum-likelihood estimation (assuming the background noise is white Gaussian) can be formulated as follows:

$$\arg_{\tilde{\tau}} \min \int \left[r(t) - \alpha s(t-\tau) \right]^2 dt \qquad (2.2)$$

where α is a function of τ . The path-loss model [10] will be discussed later in Section 2.2.2.

By neglecting the path-loss α (assuming it is a fixed constant), suboptimum

estimation can be formulated as follows:

$$\arg_{\tilde{\tau}} \min \int \left[r(t) - s(t-\tau) \right]^2 dt \qquad (2.3)$$

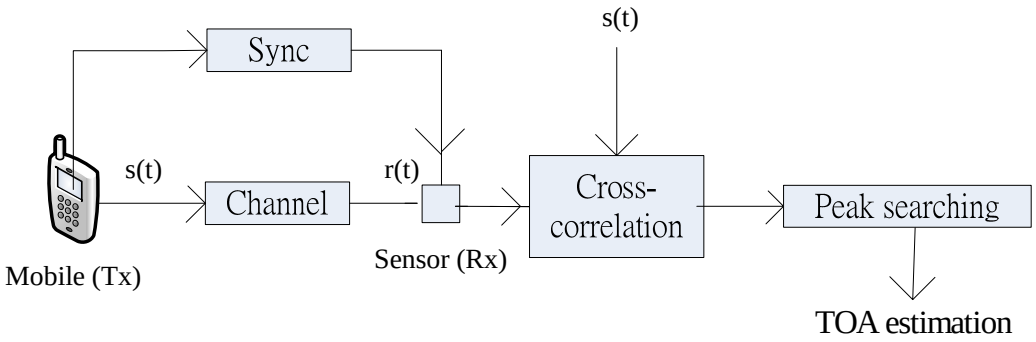

Figure 2.1 TOA estimation diagram

(2.3) can be reformulated as the famous correlator [43-44] estimation of time-delay:

$$\arg_{\tilde{\tau}} \max \int r(t)s(t-\tau)dt \qquad (2.4)$$

Fig. 2.1 illustrates the procedure of cross-correlation and peak searching. It is note that (2.4) does not consider the effect of the received signal power loss $\tilde{\alpha}$. We will incorporate both TOA and RSS techniques to propose a more accurate ranging technique in next section.

2.2.2 Ranging Scheme with a Hybrid of TOA and RSS

First, we introduce the RSS ranging technique. We assume the path-loss model is given by[10]

$$\frac{P_r}{P_0} = k_0 d^{-n_p} \qquad (2.5)$$

where P_r is the received signal power, P_0 is the transmitted signal power, d is the

true distance between transmitter and receiver, k_0 is constant, and n_p is the path-loss exponent. Once we have the parameters of P_r, k_0, n_p, and P_0 in (2.5), the distance can be estimated as follows:

$$\tilde{d} = \left(\frac{P_r}{k_0 P_0}\right)^{\frac{-1}{n_p}} \qquad (2.6)$$

Because parameters of path-loss model are sensitive to the variation of time and environment, they can affect the ranging accuracy significantly. Even they are perfectly known, RSS suffers worse degradation than correlator-based TOA method in an additive white Gaussian noise environment. Despite of the above disadvantages, the path-loss model still contains the ranging information, hence it can assist the TOA-only estimator. In the following, we will enhance TOA estimation by combining the path-loss model.

By assuming the path-loss model is known to us, we want to obtain the relationship between path-loss α and τ. In the absence of background noise, we have $P_r = \alpha^2 \int s^2(t)dt$ and $P_0 = \int s^2(t)dt$, from (2.1). By noting that $d = v\tau$, where v is the propagation speed, (2.5) becomes:

$$\alpha = \sqrt{k_0}(v\tau)^{-n_p/2} = k_1 \tau^{-n_p/2} \qquad (2.7)$$

The joint time and power estimation can be denoted as

$$\arg_{\tilde{\tau}} \min \int \left[r(t) - k_1 \tau^{-n_p/2} s(t-\tau) \right]^2 dt \qquad (2.8)$$

whose improved ranging performance will be shown in Section 5.1.

2.3 TOA (Time-of-Arrival) System Model

A localization system includes distributed sensors and a mobile. A typical localization scenario is shown in Figure 2.2. The problem is to estimate the position of mobile via the measurement from sensors. Before the mathematical formulation, the symbols are

classified as follows. (x, y) is the unknown position of mobile. (x_i, y_i) is the known position of *i*th sensor. r_i is the rage measurement between mobile and ith sensor.

Assume that there are *N* sensors available for measuring the TOAs from the mobile. The relationship between *i*th true distance and range measurements can be denoted as

$$d_i = \sqrt{(x - x_i)^2 + (y - y_i)^2} \approx r_i \qquad i = 1, 2, ..., N \qquad (2.9)$$

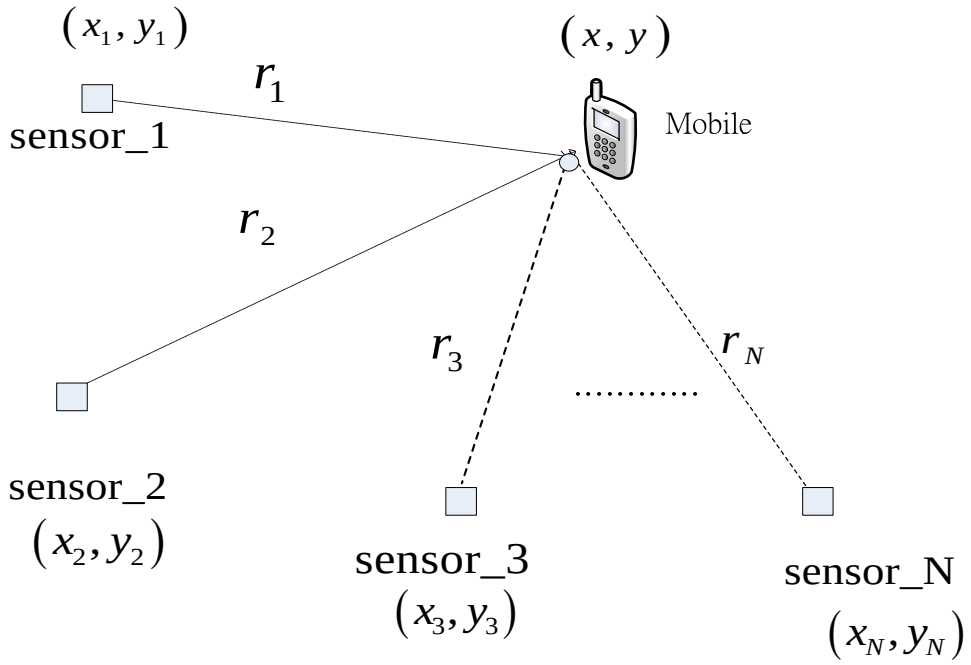

Figure 2.2 A typical localization scenario

where $r_i = d_i + n_i + L_i$. n_i is the range error for measurement of ith sensor. L_i is NLOS bias, can be modeled as Rayleigh distribution.

Here we focus on the demonstration in LOS environment, while the situation of NLOS environment will be discussed in Section 4.2. For measuring in LOS environment, the NLOS bias L_i is assumed to be zero. In other words, the range

measurement is only influenced by the range error n_i . From the range measurements and the position of distributed sensors, we want to obtain the best position estimation. If the statistical property of the range error isn't known for us, we can resort to (LSE) least-square estimation [39] which is shown as follows:

$$(\tilde{x}, \tilde{y}) = \arg_{x,y} \min \sum_{i=1}^{N} (\sqrt{(x - x_i)^2 + (y - y_i)^2} - r_i)^2 \quad (2.10)$$

In other hands, if the statistical property of the range error is known for us, we can resort to Maximum-Likelihood (ML) estimator which will be introduced in Section 2.4.

2.4 ML Estimator

The ML estimator has been derived in [40], we summarize as follows.

With the model of range error, the pdf of the range measurement of ith sensor can be denoted as

$$f_i = \frac{1}{\sqrt{2\pi\sigma_i^2}} \exp(-\frac{(r_i - d_i)^2}{2\sigma_i^2}) \qquad (2.11)$$

We assume that the range measurement between different sensors is independent, the joint pdf of all the range measurements can be denoted as:

$$p(r_1, r_2 ..., r_N) = \prod_{i=1}^{N} f_i = \frac{1}{\sqrt{2\pi}^N \sigma_1^2 \sigma_2^2 ... \sigma_N^2} \exp(-\frac{(r_1 - d_1)^2}{2\sigma_1^2} - ... - \frac{(r_N - d_N)^2}{2\sigma_N^2}) \qquad (2.12)$$

In order to maximize (2.3), the optimum solution can be shown as follows:

$$\arg \min_{(x,y)} \frac{(r_1 - d_1)^2}{2\sigma_1^2} + \frac{(r_2 - d_2)^2}{2\sigma_2^2} + ... + \frac{(r_N - d_N)^2}{2\sigma_N^2} \qquad (2.13)$$

The solution of (2.13) is also called weighted least-squares (WLS) solution [43]. Typically, the property of range error is assumed to be i.i.d, so (2.10) might be the same with (2.13). From (2.13), we can know that it is composed of non-linear terms, so we can resort to Iterative Nonlinear Least Square Solution [30]. Accurate solution

can be achieved with high cost of computation complexity. In order to save some cost, we can linearize (2.10) at first. The popular techniques of linearization will be introduced in Section 2.5.

2.5 Linearization of Least-Squares Estimator

Typical linearization techniques include hyperbolic positioning algorithm, Taylor-series based least-squares solution, distance-augmented linearization. In this section, we will introduce these techniques separately.

2.5.1. Hyperbolic Positioning Algorithm

The hyperbolic positioning algorithm [15][41] is a popular method of linear least-squares solution. We summarize the linearization techniques as follows:

(2.9) can be re-write as follows after squaring,

$$(x-x_i)^2+(y-y_i)^2 \approx r_i^2 \quad (2.14)$$

Expansion (2.14),

$$x^2+y^2-2x_i x-2y_i y+x_i^{\,2}+y_i^{\,2} \approx r_i^2 \quad (2.15)$$

where x^2+y^2 : non-linear(hyperbolic) term

We need a sensor as reference equation,

$$x^2+y^2-2x_r x-2y_r y+x_r^{\,2}+y_r^{\,2} \approx r_r^2 \quad (2.16)$$

After subtracting (2.15) form (2.16),

$$2(x_i-x_r)x+2(y_i-y_r)y \approx r_r^{\,2}-r_i^2-k_r+k_i \quad (2.17)$$

where $k_r=x_r^{\,2}+y_r^{\,2}, k_i=x_i^{\,2}+y_i^{\,2}$

We can re-write (2.17) as a matrix form as follows.

$$Ap \approx b \quad (2.18)$$

where $p=[x \;\; y]^T$ is unknown position

Where $A = \begin{bmatrix} (x_1 - x_r) & (y_1 - y_r) \\ (x_2 - x_r) & (y_2 - y_r) \\ \vdots & \vdots \\ (x_N - x_r) & (y_N - y_r) \end{bmatrix}$ $b = \begin{bmatrix} r_r^2 - r_1^2 - k_r^2 + k_1^2 / 2 \\ r_r^2 - r_2^2 - k_r^2 + k_2^2 / 2 \\ \vdots \\ r_r^2 - r_N^2 - k_r^2 + k_N^2 / 2 \end{bmatrix} = b_c + b_n$

Where $b_c = \begin{bmatrix} d_r^2 - d_1^2 - k_r^2 + k_1^2 / 2 \\ d_r^2 - d_2^2 - k_r^2 + k_2^2 / 2 \\ \vdots \\ d_r^2 - d_N^2 - k_r^2 + k_N^2 / 2 \end{bmatrix}$, $b_n = \begin{bmatrix} 2d_r n_r - 2d_1 n_1 + n_r^2 - n_1^2 / 2 \\ 2d_r n_r - 2d_2 n_2 + n_r^2 - n_2^2 / 2 \\ \vdots \\ 2d_r n_r - 2d_N n_N + n_r^2 - n_N^2 / 2 \end{bmatrix}$

We can see that the statistical property of perturbation term b_n is not i.i.d. Thus, we can apply ML weighted-least-squares solution [43] as follows:

$$\tilde{p} = (A^T W A)^{-1} A^T W b \qquad (2.19)$$

where $W = \left(E\left[b_n b_n^T \right] \right)^{-1}$, a weighted matrix.

Similarly, once we don't have the statistical property of the perturbation term, the weighting matrix can simply choose to be identity matrix.

2.5.2 Taylor-Series Approximation Method

We re-write (2.9) as follows:

$$F_i(x, y) = \sqrt{(x - x_i)^2 + (y - y_i)^2} \qquad (2.20)$$

Apply Taylor-Series expansion [42] to (2.20) as follows.

$F(x, y) = F(x_0, y_0) + [\nabla^T F(x_0, y_0)]\Delta + \text{higher order terms}$

If the reference point is close to true position enough, the higher order terms can be omitted, and (2.20) can be linearized as follows.

$$F_i(x, y) \approx F_i(x_0, y_0) + \frac{\partial F_i}{\partial x}(x - x_0) + \frac{\partial F_i}{\partial y}(y - y_0) \qquad (2.21)$$

Where $F_i(x_0, y_0) = \sqrt{(x_0 - x_i)^2 + (y_0 - y_i)^2} = d_{i,0}$ $\frac{\partial F_i}{\partial x} = \frac{x_0 - x_i}{d_{i,0}}$ $\frac{\partial F}{\partial y} = \frac{y_0 - y_i}{d_{i,0}}$

$$(\frac{x_0 - x_i}{d_{i,0}})x + (\frac{y_0 - y_i}{d_{i,0}})y \approx r_i - \tilde{d}_{i,0} \qquad (2.22)$$

Where $\tilde{d}_{i,0} = d_{i,0} - (\frac{x_0 - x_i}{d_{i,0}})x_0 - (\frac{y_0 - y_i}{d_{i,0}})y_0$

We can re-write (2.22) as a matrix form as follows.

$$H \times p = \begin{bmatrix} \frac{x_0 - x_1}{d_{1,0}} & \frac{y_0 - y_1}{d_{1,0}} \\ \frac{x_0 - x_2}{d_{2,0}} & \frac{y_0 - y_2}{d_{2,0}} \\ \vdots & \vdots \\ \frac{x_0 - x_N}{d_{N,0}} & \frac{y_0 - y_N}{d_{N,0}} \end{bmatrix} \times \begin{bmatrix} x \\ y \end{bmatrix} \approx \begin{bmatrix} r_1 - \tilde{d}_{1,0} \\ r_2 - \tilde{d}_{2,0} \\ \vdots \\ r_N - \tilde{d}_{N,0} \end{bmatrix} = b \qquad (2.23)$$

After Taylor-series approximated linearization, we can avoid the high cost of conjugate gradient, which is the main advantage of it. But before linearization, we should assure that the initial guess is good enough, or the least-squares solution might not converge after many times of iteration. In Section 3.2, we regard the hyperbolic positioning algorithm as the reference point, and will analyze the effect of it.

2.5.3 Distance-Augmented Linearization Method

The linearization method is also a popular technique in the localization field and is applied in [29]. We summaries it as follows:

From equation (2.15), let

$R = x^2 + y^2$, we can get the following equation

$$2x_i x + 2y_i y - R \approx k_i - r_i^2 \qquad (2.24)$$

We can re-write (2.24) as a matrix form as follows.

$$\begin{bmatrix} 2x_1 & 2y_1 & -1 \\ 2x_2 & 2y_2 & -1 \\ \vdots & \vdots & \vdots \\ 2x_N & 2y_N & -1 \end{bmatrix} \times \begin{bmatrix} x \\ y \\ R \end{bmatrix} \approx \begin{bmatrix} k_1 - r_1^2 \\ k_2 - r_2^2 \\ \vdots \\ k_N - r_N^2 \end{bmatrix} \quad (2.25)$$

From the derivation of above, we can realize the key is that we enable $R = x^2 + y^2$ with the degree of freedom. Equivalently, we let R be independent of x and y, so the non-linear equation can be linearized. While the linearization suffers from range error and the error of new variable R, the accuracy might be the worst one, and is seldom applied in localization. Thus, we don't focus on the analysis of theoretical error of the linearization method which is introduced in this section.

Chapter 3
Asymptotically Theoretical Error Analyses

Recent years, the analysis and comparisons of non-linear LS and linear LS solution is proposed in [15]. In [17], the closed-form error covariance has been derived for hyperbolic positioning algorithm. In our research, we focus on the analysis and comparison of different linearization techniques.

Define the location estimation error as the difference between the true position vector *p* and estimated position vector $\tilde{p}$:

$$e = p - \tilde{p}$$

Mean square error (MSE) is defined as

$$E\left[\|e\|^2\right] \qquad (3.1)$$

will be used as the performance measure of localization accuracy.

We summarize the general theoretical derivation as following.

Typical linearized LS solution has the following form:

$$\tilde{p} = (A^T A)^{-1} A^T b = (A^T A)^{-1} A^T (b_c + b_n) = p + e$$

where $b = b_c + b_n$, b_n is the error comes from range error and modeling error, and $e = (A^T A)^{-1} A^T b_n$

The error covariance can be written as following:

$$E\left[ee^T\right] = (A^T A)^{-1} A^T E\left[b_n b_n{}^T\right] A(A^T A)^{-1} \qquad (3.2)$$

The mean square error (MSE) can be written as:

$$E\left[\|e\|^2\right] = trace(E[ee^T])$$

[17] has derived the closed-form error covariance of (3.2). Obviously, the expectation is taken with respect to the range error in (3.2), while the matrix A is varied with respect to the position of sensors and mobile. In this chapter, we derived the asymptotic theoretical error of hyperbolic positioning algorithm and TS-approximated LS solution in line-of-sight environment with the increasing of sensors. We also derived the asymptotic MSE of hyperbolic positioning algorithm under weighted-least-squares solution.

3.1 Theoretical Analysis of Hyperbolic Positioning Algorithm

In this section, we introduce typical hyperbolic positioning algorithm first. In Section 3.1.1, with some assumptions, the MSE can be derived as a simpler form. Next, we further derived asymptotic MSE which is a clear equation. In Section 3.1.2 we derive the hyperbolic positioning algorithm lower bound by weighted LS solution.

3.1.1 Hyperbolic Positioning without Weighted LS

The hyperbolic positioning algorithm relies on a sensor as reference equation. So, the selection of sensor is very important for location estimation of the mobile. First, [17] choose sensor at origin as the reference terminal. But the performance will degrade when the mobile is far away from the reference sensor. In intuition, one can choose a sensor with shortest range as the reference sensor. This can improve some performance than the former method. The two reference sensor selection method is popular in the literature. However, there is a lower bound for hyperbolic positioning algorithm. In this section, we derive and analysis the lower bound of hyperbolic positioning algorithm.

From (2.18) and (3.2), the theoretical error covariance of hyperbolic positioning algorithm can be denoted as following:

$$E\left[ee^T\right] = (A^T A)^{-1} A^T E\left[b_n b_n^T\right] A(A^T A)^{-1} \quad (3.3)$$

From the derivation of [17], $E\left[b_n b_n^T\right]$ can be denoted as:

$$\begin{aligned} E[b_n b_n^T]_{ij} &= d_r^2 \sigma^2 + 1.5\sigma^4 \approx d_r^2 \sigma^2 \\ E[b_n b_n^T]_{ii} &= (d_r^2 + d_i^2)\sigma^2 + 2\sigma^4 \approx (d_r^2 + d_i^2)\sigma^2 \end{aligned} \quad (3.4)$$

where σ^2 is the variance of range error.

We can see that $E\left[b_n b_n^T\right]$ is not a diagonal form, so (3.4) will be too complex to derive. In order to get a simpler form, we assume that the matrix in (3.4) is diagonal form. In other words, the value of d_r in (3.4) is assumed to be zero (i.e. $(x, y) \approx (x_r, y_r)$). Physically, it represents that the reference sensor is always attacked to the mobile. However, it is not practical to replace a sensor next to the mobile. Only when there is a large amount of distributed sensors in the room, the effect of d_r can almost be omitted. So in the following derivation, we regard it as a lower bound of hyperbolic positioning algorithm and will analyze the theoretical error of this bound.

With such assumption, the distance between the reference sensor and mobile equals to zero approximately .Thus, $E\left[b_n b_n^T\right]$ can be denoted as:

$$E\left[b_n b_n^T\right] \approx \sigma^2 \begin{bmatrix} d_1^2 & 0 & \dots & 0 \\ 0 & d_2^2 & 0 & 0 \\ 0 & \dots & \dots & 0 \\ 0 & 0 & \dots & d_N^2 \end{bmatrix} = \sigma^2 D \quad (3.5)$$

Thus, the matrix above is a diagonal form as we want it to be.

Combined (3.3) and (3.5),

$$E\left[ee^T\right] = \sigma^2 (A^T A)^{-1} A^T D A (A^T A)^{-1} \quad (3.6)$$

The exact mathematical form of (3.6) is hard to be expressed, so we divide it into 3

blocks (i.e. $(A^T A)^{-1} \times A^T DA \times (A^T A)^{-1}$).

The first and the third block, $A^T A$ can be denoted as

$$A^T A = \begin{bmatrix} \sum_{i=1}^{N} (x_i - x_r)^2 & \sum_{i=1}^{N} (x_i - x_r)(y_i - y_r) \\ \sum_{i=1}^{N} (x_i - x_r)(y_i - y_r) & \sum_{i=1}^{N} (y_i - y_r)^2 \end{bmatrix} \quad (3.7)$$

If the number of the sensor is large enough, and also the distribution of the sensor is random enough, the x-y cross-term will approximately equal to zero. So (3.7) can be written as:

$$A^T A \approx \begin{bmatrix} \sum_{i=1}^{N} (x_i - x_r)^2 & 0 \\ 0 & \sum_{i=1}^{N} (y_i - y_r)^2 \end{bmatrix} \quad (3.8)$$

Similarly,

$$A^T DA \approx \sigma^2 \times \begin{bmatrix} \sum_{i=1}^{N} d_i^2 (x_i - x_r)^2 & 0 \\ 0 & \sum_{i=1}^{N} d_i^2 (y_i - y_r)^2 \end{bmatrix} \quad (3.9)$$

From (3.5), (3.8), and (3.9), the theoretical error can be further denoted as

$$E[ee^T \mid p] \approx \sigma^2 \begin{bmatrix} \frac{\sum_{i=1}^{N} d_i^2 (x_i - x_r)^2}{\left[\sum_{i=1}^{N} (x_i - x_r)^2\right]^2} & 0 \\ 0 & \frac{\sum_{i=1}^{N} d_i^2 (y_i - y_r)^2}{\left[\sum_{i=1}^{N} (y_i - y_r)^2\right]^2} \end{bmatrix} \quad (3.10)$$

The notation $E[ee^T \mid p]$ represent that the theoretical error is derived when the position of sensors and mobile is given. We are interested in what the theoretical error will be if the position of mobile and sensors is averaged over the room. Under the assumption that the sensors are uniformly distributed in a $L \times L$ squared room and

the mobile also locates at random position, we derive the mean of $E[ee^T \mid p]$ versus position:

$$E\left\{E[ee^T \mid p]\right\} \approx \sigma^2 \times E\left\{\begin{bmatrix} \dfrac{\sum_{i=1}^{N} d_i^{\,2}\left(x_i - x_r\right)^2}{\left[\sum_{i=1}^{N}\left(x_i - x_r\right)^2\right]^2} & 0 \\ 0 & \dfrac{\sum_{i=1}^{N} d_i^{\,2}\left(y_i - y_r\right)^2}{\left[\sum_{i=1}^{N}\left(y_i - y_r\right)^2\right]^2} \end{bmatrix}_p\right\} \qquad (3.11)$$

Assume that the expectation of divider and denominator can be taken independently, and the position of sensors and mobile $(x, y), (x_i, y_i)$ satisfies:

$x, y, x_i, y_i \sim U(0, L)$ $\quad U(0, L)$: Uniform distribution within [0,L]

The following is the calculation of the expectation of (3.11):

$$E\left[\sum_{i=1}^{N} d_i^{\,2}\left(x_i - x_r\right)^2\right] = \sum_{i=1}^{N} E\left[d_i^{\,2}\left(x_i - x_r\right)^2\right] = N \times E\left[d_i^{\,2}\left(x_i - x_r\right)^2\right]$$

$$E\left[d_i^{\,2}\left(x_i - x_r\right)^2\right] = E\left\{\left[\left(x_i - x_r\right)^2 + \left(y_i - y_r\right)^2\right]\left(x_i - x_r\right)^2\right\}$$
$$= E\left[\left(x_i - x_r\right)^4 + \left(x_i - x_r\right)^2 \times \left(y_i - y_r\right)^2\right]$$
$$= E\left[\left(x_i - x_r\right)^4\right] + E\left[\left(x_i - x_r\right)^2\right] \times E\left[\left(y_i - y_r\right)^2\right]$$
$$= \frac{L^4}{15} + \frac{L^2}{6} \times \frac{L^2}{6} = \frac{17L^4}{180}$$

$$E\left\{\left[\sum_{i=1}^{N}\left(x_i - x_r\right)^2\right]^2\right\} = \sum_{i=1}^{N}\left(x_i - x_r\right)^4 + 2 \times \sum_{i=1}^{N}\left(x_i - x_r\right)^2\left(x_j - x_r\right)^2$$

$$E\left[\left(x_i - x_r\right)^4\right] = \frac{L^4}{15}$$

$$E\left[\left(x_i - x_r\right)^2\left(x_j - x_r\right)^2\right] = \frac{L^4}{30}$$

$$E\left\{\left[\left(x_1 - x_r\right)^2 + \left(x_2 - x_r\right)^2 + \ldots\left(x_N - x_r\right)^2\right]^2\right\} = \frac{L^4}{15}N + 2 \times \frac{N(N-1)}{2} \times \frac{L^4}{30} = \frac{L^4}{30}(N^2 + N)$$

Thus, (3.9) can be simplified as follows.

$$E\left\{E[ee^T \mid p]\right\}_p \approx \sigma^2 \begin{bmatrix} \frac{17L^4N}{180} \Big/ \frac{L^4}{30}(N^2+N) & 0 \\ 0 & \frac{17L^4N}{180} \Big/ \frac{L^4}{30}(N^2+N) \end{bmatrix} \quad (3.12)$$

$$= \sigma^2 \times \frac{17}{6(N+1)} \times I$$

where I is a 2x2 identity matrix.

Finally, the asymptoticMSE can be obtained by calculating the diagonal sum of the position error covariance as following:

$$\text{asymptotic MSE}=\text{trace}\left\{E\left\{E[ee^T \mid p]\right\}_p\right\} \approx \sigma^2 \times \frac{34}{6(N+1)} = \sigma^2 \times \frac{5.67}{N+1} \quad (3.13)$$

From (3.13), we can understand that the asymptotic MSE is inversely proportional to the number of sensors..

3.1.2 Hyperbolic Positioning with Distance-De-Weighted LS

From (3.5), we can realize that the localization error is highly dependent on the distances between the mobile and sensors. In other words, if the distances are the same with each other, we can interfere that the mobile is almost locates at the geometry center, and the localization error might reach its smallest value, and vice versa. However, the derivation in Section 3.1.1 is simply a lower bound under un-weighted least-squares solution. [43] has proposed a ML (maximum-likelihood) weighted LS solution to de-weight the the effect of non-uniformly distances. But the amount of improvement of localization error is not indicated in [43] theoretically. In this section, we want to show how amount of performance can be improved.

In (2.10) the optimum weighted least-squares estimator is given by:

$$\hat{p} = (A^T WA)^{-1} A^T Wb = p + e \qquad (3.14)$$

$$\text{Where } W = \left\{ E\left[b_n b_n{}^T \right] \right\}^{-1} = \begin{bmatrix} \frac{1}{d_1{}^2} & 0 & \dots & 0 \\ 0 & \frac{1}{d_2{}^2} & 0 & \vdots \\ \vdots & 0 & \dots & 0 \\ 0 & \dots & 0 & \frac{1}{d_N{}^2} \end{bmatrix} = D^{-1} \quad (3.15)$$

where $e = (A^T WA)^{-1} A^T Wb_n$.

From (3.3) and (3.14), the localization error can be denoted as follows

$$E\left[ee^T \middle| p \right] = \sigma^2 (A^T WA)^{-1} A^T WDWA(A^T WA)^{-1} = \sigma^2 (A^T D^{-1} A)^{-1} \qquad (3.16)$$

Location error covariance:

$$E\left[ee^T \middle| p \right] = \sigma^2 \times \begin{bmatrix} \sum_{i=1}^{N} \frac{(x_i - x)^2}{d_i{}^2} & \sum_{i=1}^{N} \frac{(x_i - x)(y_i - y)}{d_i{}^2} \\ \sum_{i=1}^{N} \frac{(x_i - x)(y_i - y)}{d_i{}^2} & \sum_{i=1}^{N} \frac{(y_i - y)^2}{d_i{}^2} \end{bmatrix}^{-1} \qquad (3.17)$$

With Weighted LS solution, the amount of improvement and comparison in performance will be shown in Section 3.3.

3.2 Theoretical Analysis of TS-approximated LS Solution

In this section, we discuss the asymptotic MSE for TS-approximated LS solution. Unlike hyperbolic positioning algorithm, the accuracy of TS-approximated LS solution is related to the initial guess . The issues for initial guess are discussed in Section 3.2.1. With the inaccuracy of initial guess, the effect of the modeling error is discussed in Section 3.2.2. Because the uncertainty of modeling error, we derived the asymptotic upper bound and lower bound for TS-approximated LS solution in Section 3.2.2.

3.2.1 Initial Guess

When using Taylor-series expansion to do linearization, it is well-known that a good initial guess is very important. Or the linearization modeling error will not neglect-able. A popular technique is to regard the center of the sensors as an initial guess, after linearization we can get a roughly LS solution which can be regard as a better initial guess. After iteration, we can obtain an accurate initial guess. But we don't have any property of the initial guess, the modeling error is hard to analyze. For simplicity of error analysis, we regard the hyperbolic positioning algorithm as the initial guess. Thus, the modeling error can be derived easier. In Section 3.2.2, we will discuss about it.

3.2.2 Modeling Error

As mention in Section 2.5, the TS-approximated linearization can be denoted as follows.

$$f_i(x,y) \approx f_i(x_0,y_0) + \left(\frac{\partial f_i}{\partial x} \Big| (x,y) = (x_0,y_0) \right) \times (x - x_0) + \left(\frac{\partial f_i}{\partial y} \Big| (x,y) = (x_0,y_0) \right) \times (y - y_0) + e_{m,i} \tag{3.18}$$

where $\bar{x} \in [x_0, x], \bar{y} \in [y_0, y]$,

$$e_{m,i} = \frac{1}{2} \times \begin{bmatrix} \bar{x} - x_0 & \bar{y} - y_0 \end{bmatrix} \times H_{ess} \times \begin{bmatrix} \bar{x} - x_0 \\ \bar{y} - y_0 \end{bmatrix},$$

and

$$H_{ess} = \begin{bmatrix} \frac{\partial^2 f_i}{\partial x^2} & \frac{\partial^2 f_i}{\partial x \partial y} \\ \frac{\partial^2 f_i}{\partial y \partial x} & \frac{\partial^2 f_i}{\partial y^2} \end{bmatrix}_{(x,y)=(\bar{x},\bar{y})}$$

is the Hessian matrix.

If the initial guess (x_0, y_0) is not close to the mobile enough, the modeling error (denoted as $e_{m,i}$) will be not neglected.

After linearization and apply the LS solution,

$$\hat{p} = (H^T H)^{-1} H^T b = (H^T H)^{-1} H^T (b_c + b_n) = p + e \quad (3.19)$$

where $b_c = \begin{bmatrix} d_1 - \tilde{d}_{1,0} \\ d_2 - \tilde{d}_{2,0} \\ \vdots \\ d_N - \tilde{d}_{N,0} \end{bmatrix}$

$b_n = e_r + e_m = \begin{bmatrix} n_1 \\ n_2 \\ \vdots \\ n_N \end{bmatrix} + \begin{bmatrix} e_{m,1} \\ e_{m,2} \\ \vdots \\ e_{m,N} \end{bmatrix}$ = range error vector+modeling error vector

Assume that the range error and modeling error are independent to each other,

$$E\left[b_n b_n^T\right] = E\left[e_r e_r^T\right] + E\left[e_m e_m^T\right] = \sigma^2 I + E\left[e_m e_m^T\right] \quad (3.20)$$

The modeling error is hard to handle. First, the modeling error is different from *i*th to *j*th sensor. Second the higher order terms contains the computation of the Hessian, which involved with high cost. So we resorted to modeling error upper bound [27]. However, the upper bound of TS-approximated modeling error is too complicated, so [27] has simplified it as follows.

$$0 \le e_m^2 \le \frac{1}{2}(|\delta_x| + |\delta_y|)^2 \quad (3.21)$$

The bound above is position-dependent, we further take expectation to (3.21):

$$0 \le E\left[e_m^2\right] \le E\left[\frac{1}{2}(|\delta_x| + |\delta_y|)^2\right] \quad (3.22)$$

As mention in Section 3.2.1, we regard typical hyperbolic position algorithm as the initial guess of TS-expansion, and in Section 3.1, the closed-form MSE of the initial guess can be denoted as:

$$E\left[\delta_x{}^2+\delta_y{}^2\right]\approx\sigma^2\times\frac{q}{N}\qquad(3.23)$$

where $q\geq 5.67$.

Reasonably, we can assume that $E\left[\delta_x\right]=E\left[\delta_y\right]=\sqrt{\frac{1}{2}\times\sigma^2\times\frac{q}{N}}$

The mean upper bound can be denoted as follows.

$$E\left[\frac{1}{2}(|\delta_x|+|\delta_y|)^2\right]\approx\sigma^2\times\frac{q}{N}\qquad(3.24)$$

From (3.20) and (3.24), the upper bound of error covariance:

$$E\left[b_n b_n{}^T\right]=\left(1+\frac{q}{N}\right)\times\sigma^2\qquad(3.25)$$

From (3.3) and (3.25),

$$E\left[ee^T\right]=(H^TH)^{-1}H^TE\left[b_nb_n{}^T\right]H(H^TH)^{-1}=(1+\frac{q}{N})\times\sigma^2\times(H^TH)^{-1}\qquad(3.26)$$

From (3.26), we can understand that when the number of sensor increases, the modeling error will decrease which is a reasonable trend.

Similarly, we further take expectation to (3.26) with respect to the position of sensors and mobile as follows.

$$E\left\{E\left[ee^T\,|\,p\right]\right\}=(1+\frac{q}{N})\times\sigma^2\times E\left[(H^TH)^{-1}\right]_p\qquad(3.27)$$

In Section 2.4.2, the matrix H is denoted as follows.

$$H=\begin{bmatrix}\frac{x_0-x_1}{d_{1,0}} & \frac{y_0-y_1}{d_{1,0}}\\ \frac{x_0-x_2}{d_{2,0}} & \frac{y_0-y_2}{d_{2,0}}\\ \vdots & \vdots\\ \frac{x_0-x_N}{d_{N,0}} & \frac{y_0-y_N}{d_{N,0}}\end{bmatrix}=\begin{bmatrix}c_1 & s_1\\ c_2 & s_2\\ \vdots & \vdots\\ c_N & s_N\end{bmatrix}\qquad(3.28)$$

Because $\left|\frac{x_0-x_i}{d_{i,0}}\right|\leq 1$, $\left|\frac{y_0-y_i}{d_{i,0}}\right|\leq 1$, $\left(\frac{x_0-x_i}{d_{i,0}}\right)^2+\left(\frac{y_0-y_i}{d_{i,0}}\right)^2=1$

We assume that $\frac{x_0-x_i}{d_{i,0}}=\cos\theta_i$ $\frac{y_0-y_i}{d_{i,0}}=\sin\theta_i$

$$(H^T H)^{-1} = \begin{bmatrix} \sum_{i=1}^{N} c_i^{\,2} & \sum_{i=1}^{N} c_i s_i \\ \sum_{i=1}^{N} c_i s_i & \sum_{i=1}^{N} s_i^{\,2} \end{bmatrix}^{-1} = \begin{bmatrix} \sum_{i=1}^{N} \frac{1+\cos 2\theta_i}{2} & \sum_{i=1}^{N} c_i s_i \\ \sum_{i=1}^{N} c_i s_i & \sum_{i=1}^{N} \frac{1-\cos 2\theta_i}{2} \end{bmatrix}^{-1} \quad (3.29)$$

From (3.29), we can understand that it is somehow different from (3.7). The following are some assumptions:

(1) If N is large enough, $\sum_{i=1}^{N} c_i^{\,2} = \sum_{i=1}^{N} \frac{1+\cos 2\theta_i}{2} = \frac{N}{2} + \sum_{i=1}^{N} \frac{\cos 2\theta_i}{2} \approx \frac{N}{2}$

(2) Similarly, $\sum_{i=1}^{N} s_i^{\,2} = \sum_{i=1}^{N} \frac{1-\cos 2\theta_i}{2} = \frac{N}{2} - \sum_{i=1}^{N} \frac{\cos 2\theta_i}{2} \approx \frac{N}{2}$

(3) Also, $\sum_{i=1}^{N} c_i s_i = \sum_{i=1}^{N} \frac{\sin 2\theta_i}{2} \approx 0$

Once the assumptions above are not hold when there are fewer distributed sensors, it will be discussed in Section 4.1.

Because the initial guess is variant with the position of mobile and also N is large enough, we can assume that θ is nearly uniform distribution within $0 \sim 2\pi$. Thus the assumptions above are reasonable, and (3.29) can be simplified as follows.

$$(H^T H)^{-1} \approx \frac{2}{N} \times I \quad (3.30)$$

So, the asymptotic MSE upper bound for TS-approximated with modeling error can be written as follows.

$$\begin{aligned} trace\left\{E\left\{E\left[ee^T \mid p\right]\right\}\right\}_U &\approx (1+\frac{q}{N}) \times \sigma^2 \times trace\left\{E\left[(H^T H)^{-1}\right]_p\right\} \\ &= (1+\frac{q}{N}) \times \sigma^2 \times \frac{4}{N} \end{aligned} \quad (3.31)$$

If the initial guess of the TS expansion is almost perfect, the effect of modeling error can be neglect. In other words, only range error and position of sensors influences the localization error. (3.31) can be rewritten as follows.

$$trace\left\{E\left\{E\left[ee^T \mid p\right]\right\}\right\}_L \approx \sigma^2 \times \frac{4}{N} \quad (3.32)$$

But in practical, the modeling error always exist, the performance in (3.32) is hard to achieve for almost all situations.

3.3 Comparisons with CRLB

For comparison with the result in Section 3.1 and 3.2, we also derived the asymptotic MSE of CRLB in this section. First, the CRLB is given [17]:

$$\sigma^2{}_{CRLB} = trace\left(I(x,y)^{-1} \right) \qquad (3.33)$$

where the Fisher information matrix is given by

$$I(x,y) = \begin{bmatrix} \sum_{i=1}^{N} \frac{(x-x_i)^2}{\sigma_i^{\,2} d_i^{\,2}} & \sum_{i=1}^{N} \frac{(x-x_i)(y-y_i)}{\sigma_i^{\,2} d_i^{\,2}} \\ \sum_{i=1}^{N} \frac{(x-x_i)(y-y_i)}{\sigma_i^{\,2} d_i^{\,2}} & \sum_{i=1}^{N} \frac{(y-y_i)^2}{\sigma_i^{\,2} d_i^{\,2}} \end{bmatrix} \qquad (3.34)$$

In the assumption that the range error is i.i.d, the Fisher information can be written as

$$I(x,y) = \frac{1}{\sigma^2} \begin{bmatrix} \sum_{i=1}^{N} \frac{(x-x_i)^2}{d_i^{\,2}} & \sum_{i=1}^{N} \frac{(x-x_i)(y-y_i)}{d_i^{\,2}} \\ \sum_{i=1}^{N} \frac{(x-x_i)(y-y_i)}{d_i^{\,2}} & \sum_{i=1}^{N} \frac{(y-y_i)^2}{d_i^{\,2}} \end{bmatrix} \approx \frac{1}{\sigma^2} \times H^T H \qquad (3.35)$$

From (3.30) and (3.35), the asymptotic MSE of CRLB can be denoted as

$$E\left[\sigma^2{}_{CRLB} \right]_p = trace\left(E\left[I(x,y)^{-1} \right]_p \right) \approx \sigma^2 \times \frac{4}{N} \qquad (3.36)$$

The following are some observations:

(1) From (3.32) and (3.36), we can see that the TS-approximated LS solution without modeling error will approach to CRLB asymptotically.

(2) From (3.17) and (3.35), we can understand that the theoretical lower bound of hyperbolic positioning algorithm is the same with CRLB.

(3) From (3.31) and (3.36), we can understand that the asymptotic MSE upper bound of TS-approximated LS will approach to CRLB asymptotically which

can be shown as follows:

$$(1+\frac{q}{N+1})\times\sigma^2\times\frac{4}{N}\xrightarrow{N \text{ large enough}}\sigma^2\times\frac{4}{N} \qquad (3.37)$$

Here we do a summary about the asymptotic MSE of this chapter. The comparison is shown in Table 3.1.

Table 3.1. Comparisons of Asymptotical MSE

Hyperbolic lower bound	Uniform-weight	$\sigma^2\times\frac{5.67}{N+1}$
	Distance-de-weight	$\sigma^2\times\frac{4}{N}$
TS-approximated	With modeling error(upper bound)	$(1+\frac{q}{N})\sigma^2\times\frac{4}{N}$
	Without modeling error	$\sigma^2\times\frac{4}{N}$
CRLB	$\sigma^2\times\frac{4}{N}$	

Also, for localization applications, a user might request for a specific accuracy. So the localization equipment designer should determine how many sensors should be used in line-of-sight environment. From the derivation of asymptotic MSE for CRLB in this chapter, a designer can regard the list in Table 3.2 as a reference.

Table 3.2 A simple guide to determine the number of sensors (Assume $\sigma = 0.3m$)

Spec.	30cm (σ)	25cm (0.83σ)	20cm (0.67σ)	16cm (0.53σ)	12cm (0.4σ)	10cm (0.33σ)
$N >$	4	6	9	15	25	36

Chapter 4
Other Localization Issues

In this chapter, we will consider other localization issues. First, we focus on the issue of coverage for mobile localization in a general LOS scenario. The analysis of coverage will be discussed in Section 4.1. Second, based on [29], we proposed a simplified ML method to mitigate NLOS effect in Section 4.2. Third, typical adaptive localization using Kalman filter is engaged in high computational complexity. We proposed an adaptive localization scheme combined with TS-approximated linearization technique in Section 4.3.

4.1 Coverage Analysis of TS-approximated LS Solution

In Chapter 3, we have verified the asymptotical error analysis of linear least-squares solution. While there is a large amount of distributed sensors, the coverage problem is less important. Without loss of generality, we will discuss the coverage issue in this section while there are four sensors at corners.

Because (3.28) can be supposed to be a matrix with cosines and sins, we focus on the coverage issue of TS-approximated LS solution in this section. But TS-approximated LS solution suffers from modeling error. Although the modeling error varied with different sensors, the influence of it is limited. For analysis simplicity, we neglect the modeling error in this section. First, we parameterize (3.29) in Section 4.1.1. After some assumptions and approximations, the MSE nearly can be determined by one of the parameters. The further analysis and result will be shown in Section 4.1.2.

4.1.1 Parameterization

In (3.29), some terms can't be neglected, so (3.29) should be re-written as:

$$\sigma^2 tr\left((H^T H)^{-1}\right) = \sigma^2 tr\left(\begin{bmatrix} \frac{N}{2}\left(1+\frac{\sum_{i=1}^{N}\cos 2\theta_i}{N}\right) & \frac{N}{2}\times\frac{\sum_{i=1}^{N}\sin 2\theta_i}{N} \\ \frac{N}{2}\times\frac{\sum_{i=1}^{N}\sin 2\theta_i}{N} & \frac{N}{2}\left(1-\frac{\sum_{i=1}^{N}\cos 2\theta_i}{N}\right) \end{bmatrix}^{-1}\right), \qquad (4.1)$$

$$= \sigma^2 \times \frac{N}{\frac{N^2}{4}(1-\gamma)}$$

Where $\gamma = \left(\frac{\sum_{i=1}^{N}\cos 2\theta_i}{N}\right)^2 + \left(\frac{\sum_{i=1}^{N}\sin 2\theta_i}{N}\right)^2$

From (4.1), we can understand that the localization error is a function of σ^2, N, γ. In the case that N=4 , and σ^2 is given, the MSE can be written as

$$\text{MSE} = f(\gamma) = \sigma^2 \times \frac{1}{(1-\gamma)} \qquad (4.2)$$

4.1.2 Further Analysis

$$\text{Assume } \gamma = \left(\frac{\sum_{i=1}^{4}\cos 2\theta_i}{4}\right)^2 + \left(\frac{\sum_{i=1}^{4}\sin 2\theta_i}{4}\right)^2 = \varepsilon^2 + \delta^2 \qquad (4.3)$$

where $\varepsilon = \frac{\sum_{i=1}^{4}\cos 2\theta_i}{4}$ and $\delta = \frac{\sum_{i=1}^{4}\sin 2\theta_i}{4}$, are geometric parameters.

Figure 4.1 shows a general geometric setting scenario for N=4 . From (3.28) and the setting of Figure 4.1, the angle matrix can be written as:

$$H = \begin{bmatrix} \cos\theta_1 & \sin\theta_1 \\ \cos\theta_2 & \sin\theta_2 \\ \cos\theta_3 & \sin\theta_3 \\ \cos\theta_4 & \sin\theta_4 \end{bmatrix} = \begin{bmatrix} \cos\alpha_1 & \sin\alpha_1 \\ \cos(\pi-\alpha_2) & \sin(\pi-\alpha_2) \\ \cos(\pi+\alpha_3) & \sin(\pi+\alpha_3) \\ \cos(-\alpha_4) & \sin(-\alpha_4) \end{bmatrix} \quad (4.4)$$

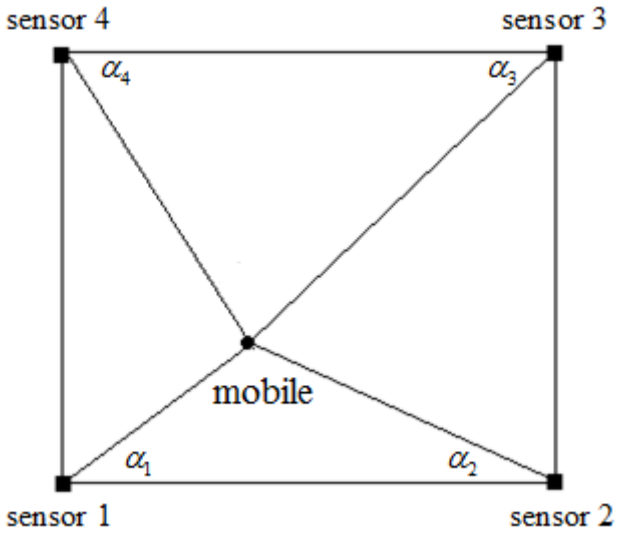

Figure 4.1 The corresponding angles from initial guess to each sensor

Generally, we can view ith sensor as original, and then the corresponding angle θ_n will locate at the quadrant of the mobile.

4.1.2.a Effect of Parameter ε

Because the sensor geometry is symmetric, if we can know the localization ability of the area displayed in Figure 4.2, we can realize the localization ability of the whole area.

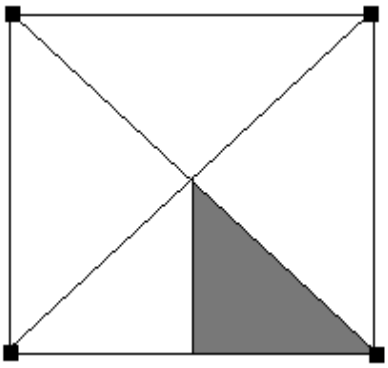

Figure 4.2 An area as a general case

We randomly choose a point in the indicated area of figure as an example. First, we focus on θ_1 and θ_3 in figure. Find point C, and then let $\overline{AB} = \overline{AC}$. From Figure 4.3, we can know that

$$\alpha_3 + \beta + \alpha_1 = \frac{\pi}{2} \qquad (4.5)$$

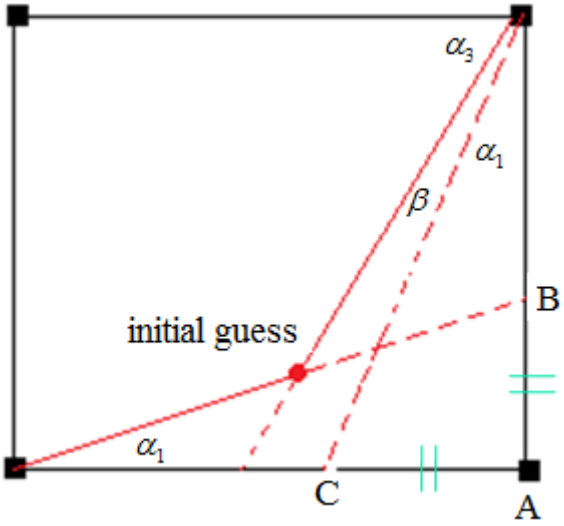

Figure 4.3 A point in a general area for sensor 1 and 3

Similarly, in Figure 4.4, we can get the relationship as follows:

$$\alpha_2 + \phi + \alpha_4 = \frac{\pi}{2} \qquad (4.6)$$

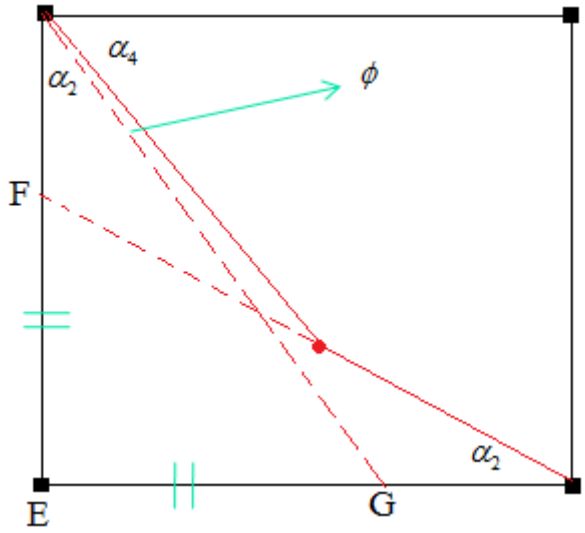

Figure 4.4 A point in a general area for sensor 2 and 4.

From (4.5) and (4.6),

$$\begin{aligned} \theta_1 + \theta_3 &= \alpha_1 + (\pi + \alpha_3) = \pi + (\alpha_1 + \alpha_3) = \frac{3}{2}\pi - \beta \\ \theta_2 + \theta_4 &= \pi - \alpha_2 - \alpha_4 = \pi - (\alpha_2 + \alpha_4) = \frac{\pi}{2} + \phi \end{aligned} \qquad (4.7)$$

where $\beta,\ \phi \geq 0$

From (4.7), the value of ε can be written as

$$\begin{aligned} \varepsilon &= \frac{\cos 2\theta_1 + \cos 2(\frac{3}{2}\pi - \theta_1 - \beta) + \cos 2\theta_2 + \cos 2(\frac{\pi}{2} - \theta_2 + \phi)}{4} \\ &\approx \frac{\sin 2\theta_1 \times 2\beta - \sin 2\theta_2 \times 2\phi}{4} = \frac{\sin 2\theta_1 \times \beta - \sin 2\theta_2 \times \phi}{2} \end{aligned} \qquad (4.8)$$

In (4.8), if the value of β and ϕ is small enough, the effect of ε is nearly not exist. From Matlab experiment, the mean value of β and ϕ is shown as follows. mean=5.9613° , std=5.5048° . Thus, the geometric parameter ε almost can be neglected.

4.1.2.b Effect of Parameter δ

Similarly, form (4.7), the value of δ can be written as

$$\begin{aligned}\delta &= \frac{\sin 2\theta_1 + \sin 2(\frac{3}{2}\pi - \theta_1 - \beta) + \sin 2\theta_2 + \sin 2(\frac{\pi}{2} - \theta_2 + \phi)}{4} \\ &\approx \frac{\sin 2\theta_1 + \sin 2\theta_2 + \beta \times \cos 2\theta_1 - \phi \times \cos 2\theta_1}{2}\end{aligned} \quad (4.9)$$

In (4.9), we can understand that even if the value of β and ϕ is small enough, the value of δ will be influenced by the value of $\sin 2\theta_1$ and $\sin 2\theta_2$. Thus, the MSE is nearly depend on the value of δ. In other words, (4.2) can be re-written as following:

$$MSE \approx f(\delta) = \sigma^2 \times \frac{1}{\left(1-\delta^2\right)} \quad (4.10)$$

In Chapter 5, it will be shown in our simulation.

4.2 NLOS Mitigation by Simplified ML Solution

When the direct path between the propagation from mobile to sensor is not existed, the measurement error is so-called NLOS error which is shown in Figure 4.5. Intuitionally, the measured distance of the third sensor would be too long which resulted in degrading on localization performance. NLOS propagation error mitigation is still a popular issue to be solved. General NLOS error mitigation includes of two parts:

(1). NLOS identification [26]: In the measurements, we should identify which sensor suffers from NLOS bias.

(2). NLOS mitigation [29]: With the identification of NLOS bias, we should apply signal processing techniques to mitigate the error caused by NLOS bias.

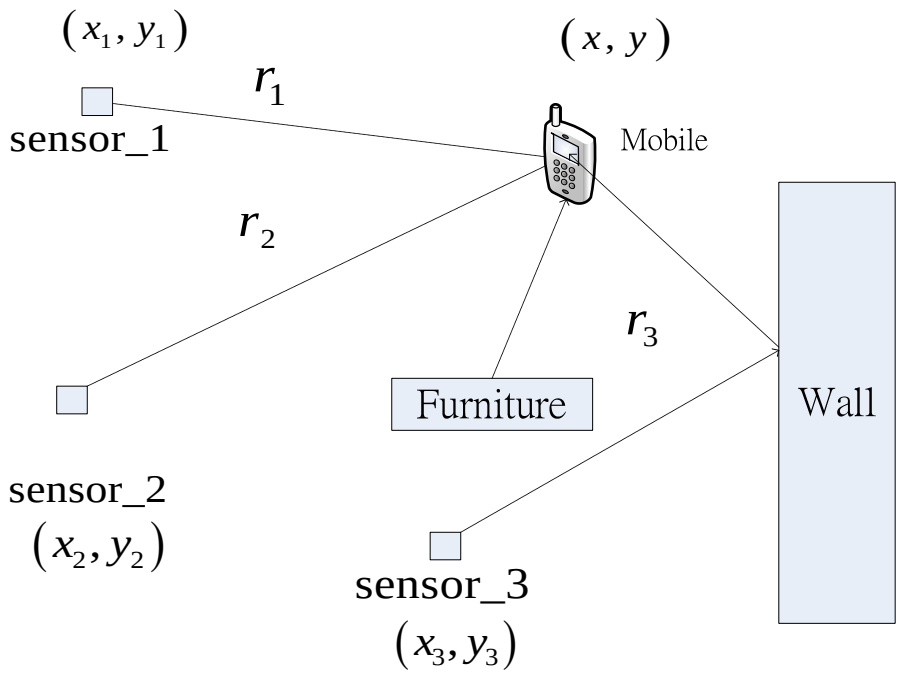

Figure 4.5 The occurrence of NLOS effect

In this section, we assume that the identification of NLOS sensor has been done and will focus on the NLOS mitigation. In Section 4.2.1 we formulate the problem of NLOS effect. An optimum solution based on statistics is proposed and derived in [29]. We summarize it in Section 4.2.2. Based on [29], we proposed a simplified ML solution to mitigate NLOS effect in Section 4.2.3.

4.2.1 NLOS Problem Formulation

Once the NLOS effect had been identified by the methods proposed in [29], we assume there are m NLOS and N-m LOS sensor measurement, the mathematical equation can be denoted as follows:

$$r_i = \begin{cases} d_i + n_i & \text{for } i = 1, 2, \ldots N - m \\ d_i + n_i + L_i = d_i + \varepsilon_i & \text{for } i = N - m + 1, \ldots, N \end{cases} \quad (4.11)$$

where L_i is NLOS bias which is a positive bias, $d_i = \sqrt{(x - x_i)^2 + (y - y_i)^2}$, and $\varepsilon_i = n_i + L_i$.

(4.11) follows the model given in (2.1), while (2.1) does not consider NLOS bias. With the range measurements in (4.11), we can simply apply least-squares estimation to estimate the position of the mobile. While the accuracy might be very poor because the high residual errors from sensors with NLOS effect. The optimum solution based on statistics is proposed in [29], and we will summarize it in Section 4.2.2.

4.2.2 Optimum ML Solution

With the assumption that the measurement error and NLOS bias can be modeled as zero-mean normal distribution and Rayleigh distribution respectively, the joint distribution of the two random variables can be derived as

$$P_{\varepsilon_i} = \frac{1}{\sqrt{2\pi}\sigma_{S_i}^{\ 2}/\sigma_{n_i}} \exp\left(-\frac{\varepsilon_i^{\ 2}}{2\sigma_{n_i}^{\ 2}}\right) + \frac{\varepsilon_i}{\sigma_{S_i}^{\ 2}/\sigma_{L_i}} \exp\left(-\frac{\varepsilon_i^{\ 2}}{2\sigma_{S_i}^{\ 2}}\right) Q\left(-\frac{\varepsilon_i}{\sigma_{S_i}\sigma_{n_i}/\sigma_{L_i}}\right) \quad (4.12)$$

where $Q(.)$ is the standard Q-function and $\sigma_{S_i} = \sqrt{\sigma_{n_i}^{\ 2} + \sigma_{L_i}^{\ 2}}$. σ_{n_i} is the standard deviation of measurement error from ith sensor. σ_{L_i} is the parameter of Rayleigh distribution from ith NLOS sensor.

Define the position vector and measurement vector respectively as

$$p = [x \;\; y]^T$$

$$\boldsymbol{r} = [r_1 \;\; r_2 \cdots r_N]^T$$

The log-likelihood function $\Lambda(\boldsymbol{r} \,|\, p)$ can be denoted as

$$\Lambda(\boldsymbol{r}\,|\,p)=\int_{\text{for all }\varepsilon}\Lambda(\boldsymbol{r}\,|\,p,\varepsilon)P_{\varepsilon}(\varepsilon)d\varepsilon \quad (4.13)$$

where $P_{\varepsilon}(\varepsilon)=\prod_{i=N-m+1}^{N}P_{\varepsilon_i}(\varepsilon_i)$, $\varepsilon=\left[\varepsilon_{N-m+1},\varepsilon_{N-m+2},...,\varepsilon_N\right]$

From the derivation of [29], (4.13) can be simplified as follows.

$$\Lambda(\boldsymbol{r}\,|\,p)=\sum_{i=1}^{N-m}-\frac{(r_i-d_i)^2}{2\sigma_{n_i}^{\ 2}}+\sum_{i=N-m+1}^{N}\ln\left\{\begin{array}{l}\frac{\sigma_{n_i}}{\sqrt{2\pi}}\exp\left(-\frac{(r_i-d_i)^2}{2\sigma_{n_i}^{\ 2}}\right)+\frac{\sigma_{Li}}{\sigma_{S_i}}(r_i-d_i)\times\\ \exp\left(-\frac{(r_i-d_i)^2}{2\sigma_{S_i}^{\ 2}}\right)Q\left(-\frac{r_i-d_i}{\sigma_{S_i}\sigma_{n_i}/\sigma_{L_i}}\right)\end{array}\right\} \quad (4.14)$$

The position estimation is produced by maximizing the above log likelihood. Equivalently, the optimal estimation is achieved by:

$$\arg_p\min\left[-\Lambda(\boldsymbol{r}\,|\,p)\right] \quad (4.15)$$

Although the result of (4.15) is an optimum solution, the computation cost of iterative least-squares solution is very high. First, we adapt (4.13) as follows:

$$\Lambda(r\,|\,p)=\int_{\text{for all }\tilde{L}}\Lambda(r\,|\,p,\tilde{L})P_L(\tilde{L})d\tilde{L} \quad (4.16)$$

Where $\Lambda(r\,|\,p,\tilde{L})=k_1-\left[\left(\sum_{i=1}^{N-m}\frac{(r_i-d_i)^2}{2\sigma_{n_i}^{\ 2}}\right)+\left(\sum_{i=N-m+1}^{N}\frac{(r_i-d_i-\tilde{L}_i)^2}{2\sigma_{n_i}^{\ 2}}\right)\right]$

$k_1=N\ln\left(\frac{\sigma_{n_i}}{\sqrt{2\pi}}\right)$

$P_L(\tilde{L})=\prod_{i=N-m+1}^{N}\frac{\tilde{L}_i}{\sigma_{L_i}^{\ 2}}e^{-\frac{\tilde{L}_i^2}{2\sigma_{L_i}^{\ 2}}}$, the probability of occurrence of $\tilde{L}$

$\tilde{L}=\left[\tilde{L}_{N-m+1},\tilde{L}_{N-m+2},\tilde{L}_N\right]$, which is a vector of estimated NLOS bias.

Under the assumption, the optimal estimation is achieved by (4.15). Similarly, the computation cost of solving (4.15) is very high; we will resort to another solution with low computation complexity based on (4.16) in Section 4.2.3.

4.2.3. Simplified ML solution

Briefly, the ML estimator does a global search for all probable NLOS bias combination, while the computational cost is inevitably high. If we merely take a most probable NLOS bias combination into consideration, and according to (4.16) and (4.17), the criteria can be denoted as follows.

$$\arg_p \ \min \left[-\Lambda(r \left| p, \tilde{L}) \times P_L\left(\tilde{L}\right) \right] \quad (4.17)$$

Equivalently, (4.17) is a problem of minimizing $-\Lambda_2(r \left| p, \tilde{L}\right.)$ with a certain combination of NLOS bias estimation. The NLOS mitigation algorithm proposed in [29] estimate a probable combination of NLOS bias in the beginning. Thus, the minimization problem is equivalent with (4.17). But the NLOS bias estimation in [29] is not generated based on theoretical derivation. In other words, the NLOS bias estimated in [29] is not always reliable. In order to further enhance localization performance in NLOS environment, we consider another probable combination of NLOS bias. Thus, proposed diagram is shown in Figure 4.6, and the minimization problem can be adapted as follows:

$$\arg \ \max \left[\Lambda(r \left| p, \tilde{L}_1) \times P_L\left(\tilde{L}_1\right) + \Lambda(r \right| p, \tilde{L}_2) \times P_L\left(\tilde{L}_2\right) \right] \quad (4.18)$$

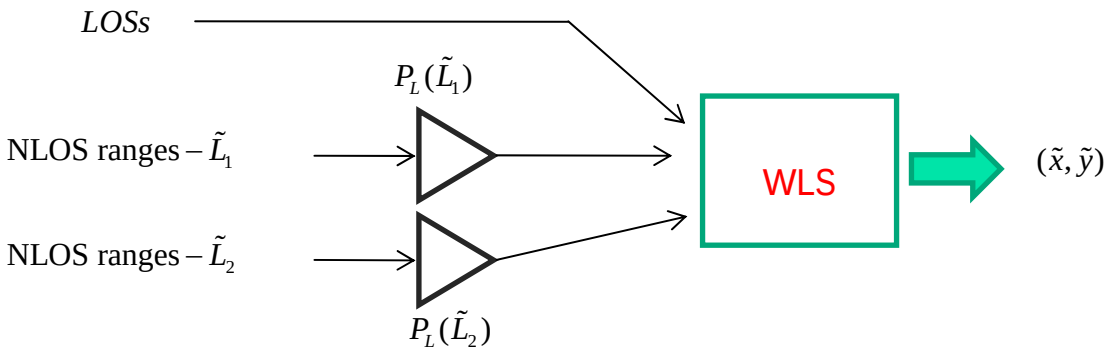

Figure 4.6 Proposed NLOS mitigation algorithm

where $\tilde{L}_1$ is a vector of NLOS bias estimation from [29], and $\tilde{L}_2$ is a vector of another probable NLOS bias estimation which may comes from the mean value of NLOS bias .

Briefly, (4.18) maximizing weighted sum of two probable likelihood functions which will be more robust than (4.17).

We summarize the NLOS bias estimation in [29] as follows.

In the beginning, an initial estimation (x_0, y_0) is generated by these original N range measurements via linear least-squares solution. For NLOS sensors, we can re-calculate the distance between the initial estimation and the position of NLOS sensors. We denoted the distance as follows:

$$\tilde{r}_i = \sqrt{(x_0 - x_i)^2 + (y_0 - y_i)^2} \quad \text{for } i = N - m + 1, ..., N \qquad (4.19)$$

We have an initial position estimation, combined with the re-calculated distance for NLOS and original measurement for LOS, the position can be estimated by TS-approximated LS solution. Equivalently, the NLOS mitigation algorithm in [29] somehow estimates the magnitude of NLOS bias. The estimated bias can be denoted as:

$$\tilde{L}_{1,i} = r_i - \tilde{r}_i \quad \text{for } i = N - m + 1, ..., N \qquad (4.20)$$

The estimation of another probable NLOS bias would be a crucial problem. Here we supply two kinds of method to be the NLOS estimation. First, the magnitude around true mean of NLOS bias may be the most probable bias statistically. A kind of probable NLOS bias can be denoted as follows:

$$\tilde{L}_{2,i} = E[L_i] \quad \text{for } i = N - m + 1, ..., N \qquad (4.21)$$

Similar to (4.21), another on-line estimation of mean of NLOS bias can be denoted as follows:

$$\tilde{L}_{3,i} = E\left[\tilde{L}_{1,i}\right] \quad \text{for } i = N - m + 1, \ldots, N \qquad (4.22)$$

From (4.18), (4.20), and (4.21), and the probability density functions of range error and NLOS bias, (4.18) can be re-written as:

$$\arg\ \min \left\{ \begin{array}{l} \left[\sum_{i=1}^{N-m} (r_i - d_i)^2 + \sum_{i=N-m+1}^{N} (r_i - d_i - \tilde{L}_{1,i})^2 - k_1 \right] \times P_L\left(\tilde{L}_1\right) + \\ \left[\sum_{i=1}^{N-m} (r_i - d_i)^2 + \sum_{i=N-m+1}^{N} (r_i - d_i - \tilde{L}_{2,i})^2 - k_1 \right] \times P_L\left(\tilde{L}_2\right) \end{array} \right\} \qquad (4.23)$$

We further simplified (4.23) as follows:

$$\arg_p\ \min \left\{ \begin{array}{l} \left[\sum_{i=1}^{N-m} (r_i - d_i)^2 + \sum_{i=N-m+1}^{N} (r_i - d_i - \tilde{L}_{1,i})^2 \right] \times P_L\left(\tilde{L}_1\right) + \\ \left[\sum_{i=1}^{N-m} (r_i - d_i)^2 + \sum_{i=N-m+1}^{N} (r_i - d_i - \tilde{L}_{2,i})^2 \right] \times P_L\left(\tilde{L}_2\right) \end{array} \right\} \qquad (4.24)$$

While k_1 is independent of p.

(4.24) can be re-written as:

$$\arg\ \min \left\{ E_1 \times P_L\left(\tilde{L}_1\right) + E_2 \times P_L\left(\tilde{L}_2\right) \right\} \qquad (4.25)$$

Where $E_1 = \sum_{i=1}^{N-m} (r_i - d_i)^2 + \sum_{i=N-m+1}^{N} (r_i - d_i - \tilde{L}_{1,i})^2$

$E_2 = \sum_{i=1}^{N-m} (r_i - d_i)^2 + \sum_{i=N-m+1}^{N} (r_i - d_i - \tilde{L}_{2,i})^2$

After TS-approximated linearization, problem in (4.25) can be denoted as a cascaded LS formulation as follows,

$$\begin{bmatrix} \sqrt{P_L\left(\tilde{L}_1\right)} \times I & 0 \\ 0 & \sqrt{P_L\left(\tilde{L}_2\right)} \times I \end{bmatrix} \begin{bmatrix} H \\ H \end{bmatrix} \times p \approx \begin{bmatrix} \sqrt{P_L\left(\tilde{L}_1\right)} \times I & 0 \\ 0 & \sqrt{P_L\left(\tilde{L}_2\right)} \times I \end{bmatrix} \times \begin{bmatrix} h_1 \\ h_2 \end{bmatrix} \qquad (4.26)$$

where H h_1 h_2 has been defined in Section 2.5.

The problem of (4.26) can be solved by the following LS solution:

$$\hat{p} = (B^T B)^{-1} B^T h \qquad (4.27)$$

where $B = \begin{bmatrix} \sqrt{P_L\left(\tilde{L}_1\right)} \times H \\ \sqrt{P_L\left(\tilde{L}_2\right)} \times H \end{bmatrix}$, $h = \begin{bmatrix} \sqrt{P_L\left(\tilde{L}_1\right)} \times h_1 \\ \sqrt{P_L\left(\tilde{L}_2\right)} \times h_2 \end{bmatrix}$

Similarly, if we want to rely on the on-line mean bias estimation, we can combine (4.18) and (4.21). The minimization criteria can be denoted as follows:

$$\arg\ \min \left\{ E_1 \times P_L\left(\tilde{L}_1\right) + E_2 \times P_L\left(\tilde{L}_3\right) \right\} \quad (4.28)$$

(4.28) can be solved by (4.27) similarly. The simulation results of proposed simplified ML of NLOS mitigation will be presented and discussed in Chapter 5.

4.3 Adaptive Localization of Moving Mobiles

In this section, we introduce conventional adaptive position update using Kalman filter in Section 4.4.1. In Section 4.4.2, we simplified the conventional Kalman gain and obtain a simple adaptive update of position estimation. In Section 4.4.3, we will propose an adaptive localization scheme under NLOS environment.

4.3.1 Adaptive Position Update Using Kalman Filter

The Kalman filter [34][35] addresses the general problem of estimating the state of a discrete-time process that is governed by the linear stochastic difference equation

$$p_k = Ap_{k-1} + Bu_{k-1} + w_{k-1} \quad (4.29)$$

With the measurement $z_k \in R^N$ that is

$$z_k = Hp_k + v_k \quad (4.30)$$

The random variables w_k and v_k represent the process and measurement noise (respectively). They are assumed to be independent to each other, white, and with normal probability distributions

$$p(w) \sim N(0, Q)$$
$$p(v) \sim N(0, R) \qquad (4.31)$$

In (4.30), if we apply TS-approximated linearization, the matrix H is the same with (2.14).

The specific procedure for update of parameter is presented below in Figure 4.7.

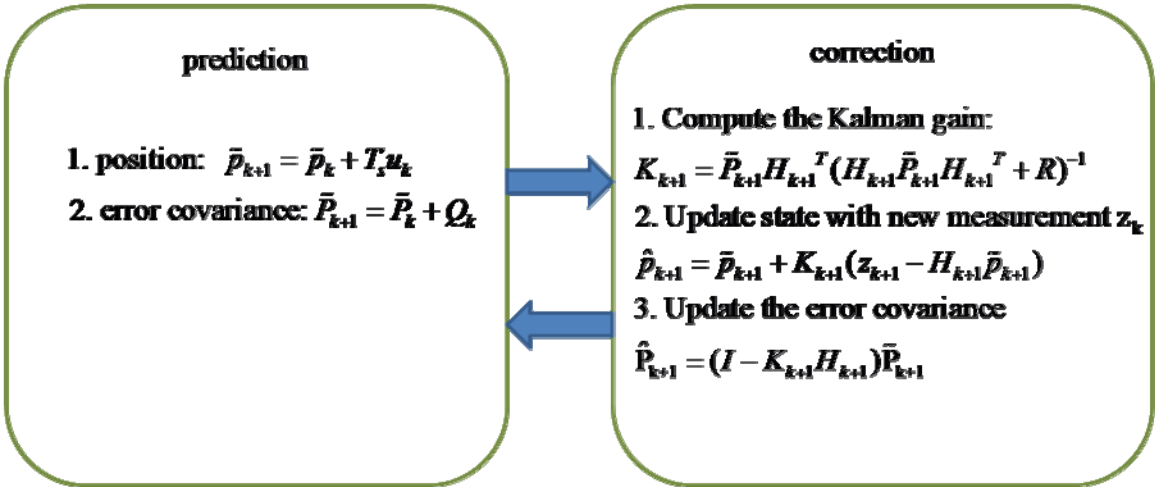

Figure 4.7 Diagram of a Kalman filter, adapted from [34]

where $P_k = E\left[e_k e_k^T\right]$, which is *a posteriori* estimate error covariance

$$e_k = p_k - \tilde{p}_k$$

From Figure 4.7, we can understand that the high computation of cost of the part of correction. In Section 4.3.2, our goal is to simplify the part of correction and compare the difference of performance.

4.3.2 Adaptive Position Update Using Simplified Kalman Filter

First, we focus on the simplification of the Kalman gain. If the SNR is higher than a general level, the error covariance matrix R nearly can be neglected. So the correction part in Figure 4.7 can be modified as below in Figure 4.8

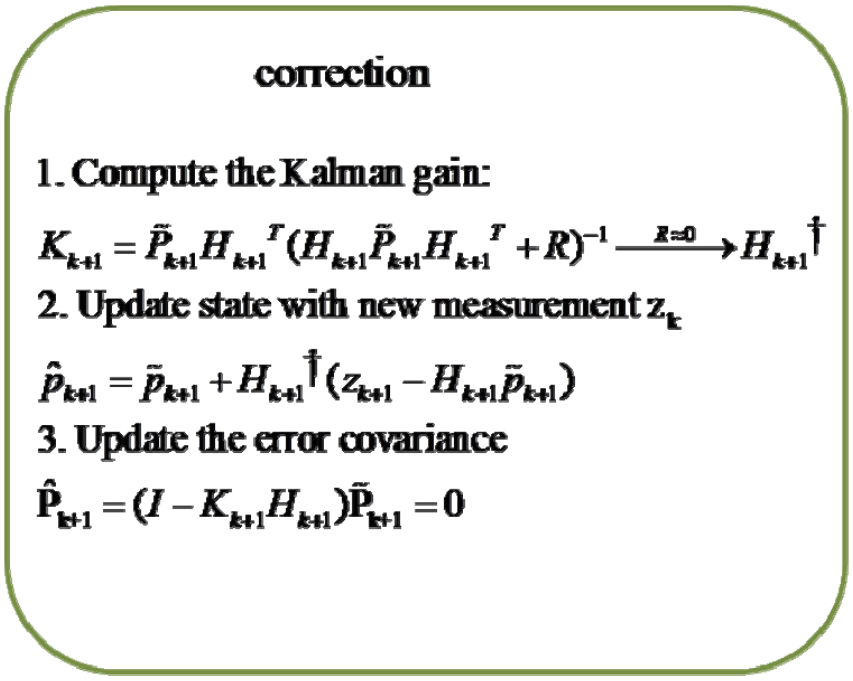

Figure 4.8 Simplified Kalman filter

From Figure 4.8, we can understand that the computational complexity of Kalman gain is highly reduced. Furthermore, if we apply TS-approximated linearization to observations, the position update equation can be simplified as follows:

$$p_{k+1} = p_k + H_{k+1}^{\dagger}(r_{k+1} - \overline{r}_k) \qquad (4.32)$$

where r_{k+1} is a range measurement vector at time index $k+1$. $\overline{r}_k$ is a distance vector which is calculated from prediction position and position of the sensors.

With the simplified Kalman gain, the error covariance is unexpected closed to zero which is not an ideal result. This might degrade some performance. Meanwhile, when the SNR is no longer good enough, the approximation in Figure 4.8 may no longer hold. This effect will be discussed and shown in our simulation in Chapter 5.

4.3.3 Adaptive Localization in NLOS Environment

For the tracking of a mobile, we will have information of consecutive range measurements. Between two closed range measurements, the range difference might

bounded by a certain amount. We utilize this property and attempt to enhance the accuracy of adaptive localization in NLOS environment. From (4.14), we can understand that magnitude of all elements of $\overline{r}_k$ and r_{k+1} might comparable. So we detect the occurrence of NLOS by the following description:

$$\text{If } \; r_{k+1,i} - \overline{r}_{k,i} > T \quad \text{We infer that NLOS error occurred.} \quad (4.33)$$

where T is a threshold, related to the magnitude of NLOS bias.

Once we infer that the measurement suffered from NLOS bias error at time index k+1, we replace r_{k+1} as follows:

$$r_{k+1} = \lambda r_k + (1-\lambda) r_{k+1} \quad (4.34)$$

where λ is a forgetting factor. Usually, $\lambda = 0.9 \sim 1$.

Because NLOS bias error may occur with a certain period typically, the forgetting factor avoids that the range would stop updating with a long time. The simulation result will be shown in Chapter 5.

Chapter 5
Computer Simulations

We will show the simulations of Chapters 3 and 4 to verify the algorithms in this chapter. In Section 5.1 we show the proposed range estimation of joint time and power technique. In Section 5.2 and 5.3, we verify the theoretical analysis derived in Chapter 3. The result of coverage analysis will be shown in Section 5.4. Section 5.5, compares the proposed two NLOS mitigation algorithms and the method in [29]. Finally, in Section 5.6, we will compare the proposed tracking technique by simplified Kalman filter with conventional one.

The performance measure for localization evaluation is:

$$\text{RMSE(Root-Mean-Square-Error)} = \sqrt{MSE} = \sqrt{E[\|e\|^2]} \qquad (5.1)$$

where $e = p - \tilde{p}$ is the location estimation error defined in (3.1) 1000 independent trials are performed for each simulation of MSE.

5.1 Simulations of Range Measurement

In this section, we show the simulations of range estimations. First, we simulate conventional correlation scheme in Section 5.1.1. Localization accuracy is highly dependent on accurate measurement. The simulation result of proposed range estimation by joint time/power scheme will present in Section 5.1.2.

5.1.1 Conventional TOA estimator

In this section, we introduce and simulate correlator-based TOA estimator [44]. The selection of signal is an important issue. Chirp signal (or PN sequence) has the

property of high processing gain and its auto-correlation has a high peak and narrow width. These properties make it be regarded as a proper transmitted signal. We can see the advantage of these properties in the following discussion and Figures. The parameter we simulated is described as follows. The transmitted signal in Section 5.1 is a chirp signal with duration 1 second and bandwidth 500Hz. The sampling rate is 1000Hz.

The true distance between mobile and sensor is 35m. We assume that the speed of sound is 350m/s. We assume the gain of direct path is α_1 and there is a multipath signal (with power gain $0.7\alpha_1$) which followed the direct path. The received signal can be denoted as

$$r(t) = \alpha_1 s(t-\tau) + \alpha_2 s(t-\tau_m) + n(t) \quad (5.2)$$

We assume $\tau = 100$ (sampling period), and $\tau_m = 110$. The normalized correlation output is shown in Figure 5.1.

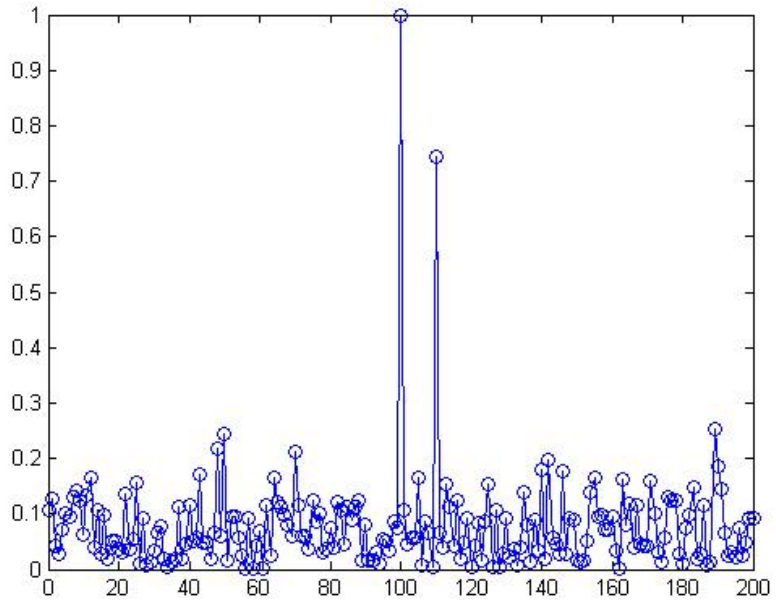

Figure 5.1 Normalized correlation output(Chirp duration=1 sec or 1000 samples)

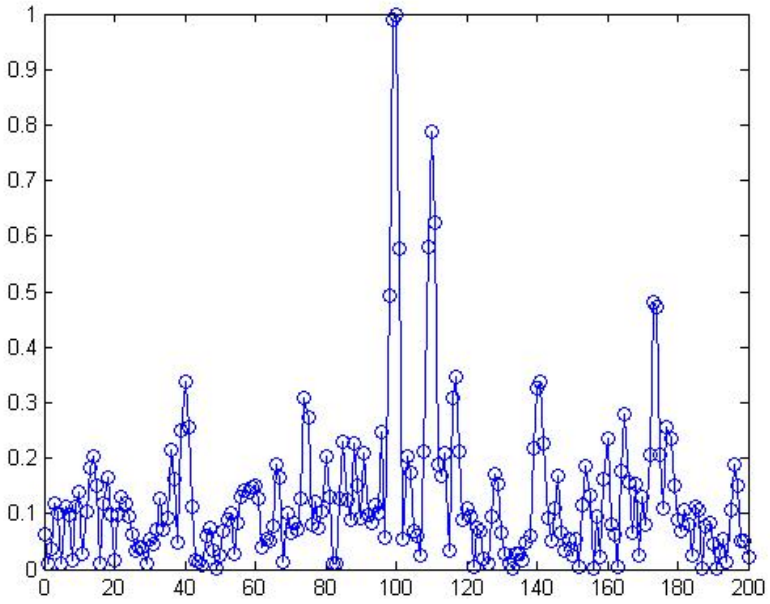

Figure 5.2 Normalized correlation output (Chirp duration=0.4 sec or 400 samples)

Once we set a threshold (for example, 0.7), the time-of-arrival of direct path can be estimated. If we choose a chirp signal with duration 0.4 second (a shorter one) and bandwidth 500Hz, the normalized correlation output is shown in Figure 5.2. We can understand that the two lobes of correlation output near the true TOA at 100 samples would broaden. If the multipath is much closer to the direct path, we can imagine that the two lobes will interfere with each other. This situation result in TOA estimation error. So a chirp signal (or PN sequence) with long duration (high processing gain) is a good choice of transmitted signal.

We further discuss the importance of the property of transmitted signal as follows. The cross-correlation is highly dependent on the auto-correlation of $s(t)$. We show the autocorrelation output with respect to different chirp signal duration in Figure 5.3.

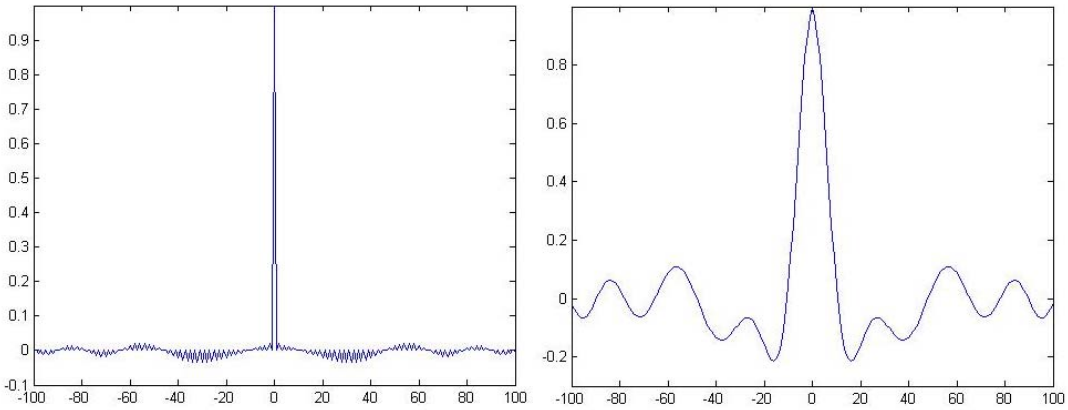

Figure 5.3 Auto correlation output (left: duration=1 sec, right: duration=0.4 sec)

From Figure 5.3, we can understand that a chirp signal with long duration (high processing gain) would have better autocorrelation property. As shown in Figure 5.3, a chirp signal with higher processing gain will have better resolution in time.

In the other hand, SNR (Signal to Noise Ratio) is another factor which affects the accuracy of TOA estimation. Figure 5.4 shows the simulation result of the TOA estimation with respect to SNR (Signal to Noise Ratio). A point in the Figure comes from 10000 times of estimations. The performance evaluation is the standard deviation of range error. From Figure 5.4, we obtain two observations. First, the ranging accuracy improves with increased SNR. Second, a chirp signal with longer duration will have better performance.

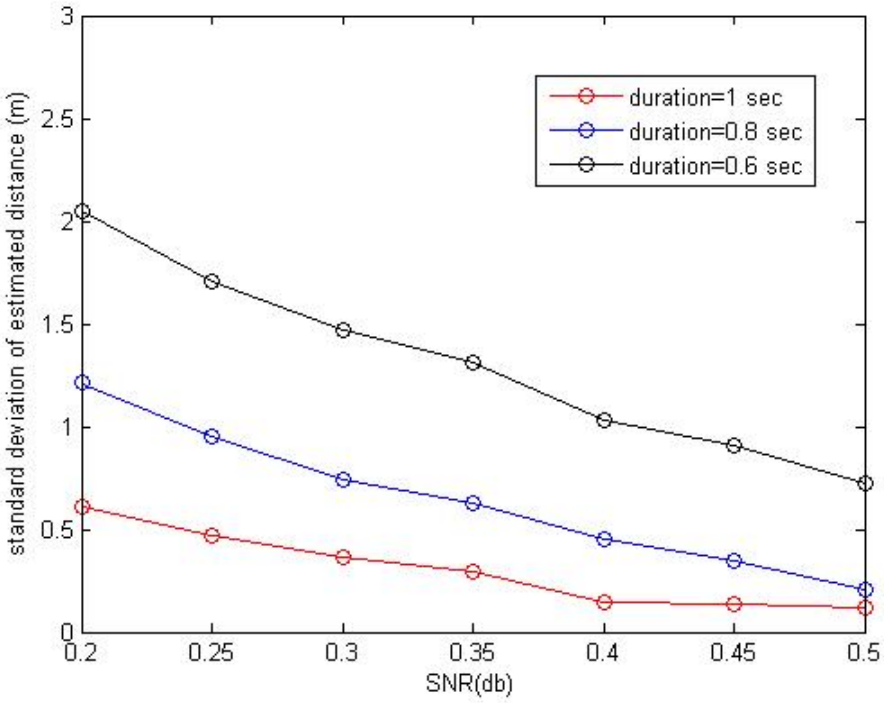

Figure 5.4 Standard deviation of range error v.s. SNR

5.1.2 Ranging Technique by a Hybrid of TOA and RSS

We assume that there is only a direct path, and the path-loss model $k_1 = 2$, $n = 2$, in (2.7). We can see from Figure 5.5 that RSS performance is the poorest one, the correlator follows next, and the hybrid outperforms the others.

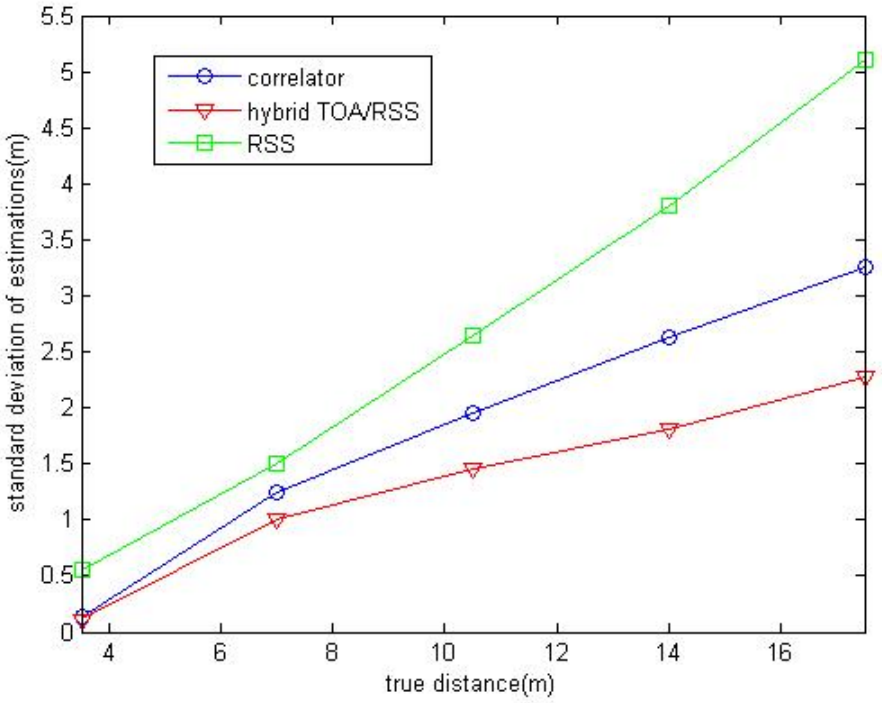

Figure 5.5 Standard deviation of range error v.s. true distance

5.2 Asymptotic MSE of Hyperbolic Positioning Algorithm

In Sections 5.2-5.3, we assume the sensors are distributed randomly and the mobile locates at the room randomly for 1000 times in a $6m \times 6m$ room. The range error is normal distributed random variable with standard deviation $\sigma = 10cm$.

As mention in Section 3.1, the performance is highly dependent on the reference sensor selection. Figure 5.6 shows the performance distinction, we can see the result as follows.

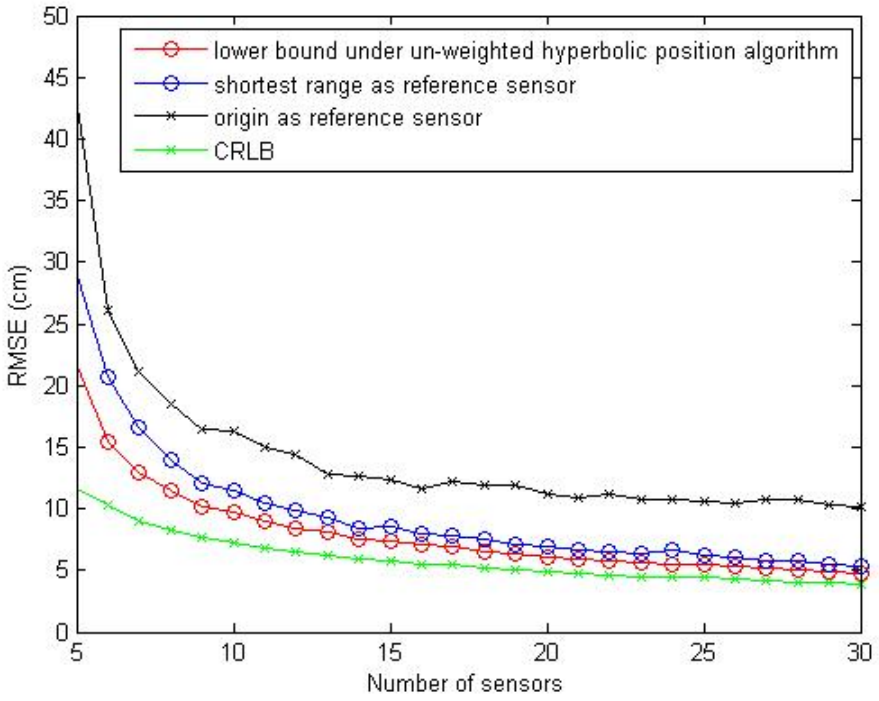

Figure 5.6 Different reference sensor selections

First, if we always choose the sensor which locates at origin, as mention in [17], the performance might degrade as the mobile far away from origin. Only when the mobile terminal always moves around the origin, the performance may acceptable. Or the performance will highly degrade. Second, if we choose the shortest range measurement as reference sensor, the performance might be enhanced about 5cm (0.5σ). Besides, the red line is a theoretical result which can't be achieved practically because it assumed that the shortest range is zero. However, if the there is a large amount of distributed sensors in the room, the blue line will approach to the red line asymptotically. In addition, the lowest line is the result of CRLB, which is hard to achieve.

The red line comes from (3.6), and based on (3.6) we have derived a asymptotic MSE in (3.13). In Figure 5.7 we show the comparison of (3.6) and (3.13) theoretically.

For comparison, we re-write them as follows:

$$\text{Closed-form MSE: } \sigma^2 \times (A^T A)^{-1} A^T DA (A^T A)^{-1} \qquad (5.3)$$

$$\text{Asymptotic MSE: } \sigma^2 \times \frac{5.67}{N+1} \qquad (5.4)$$

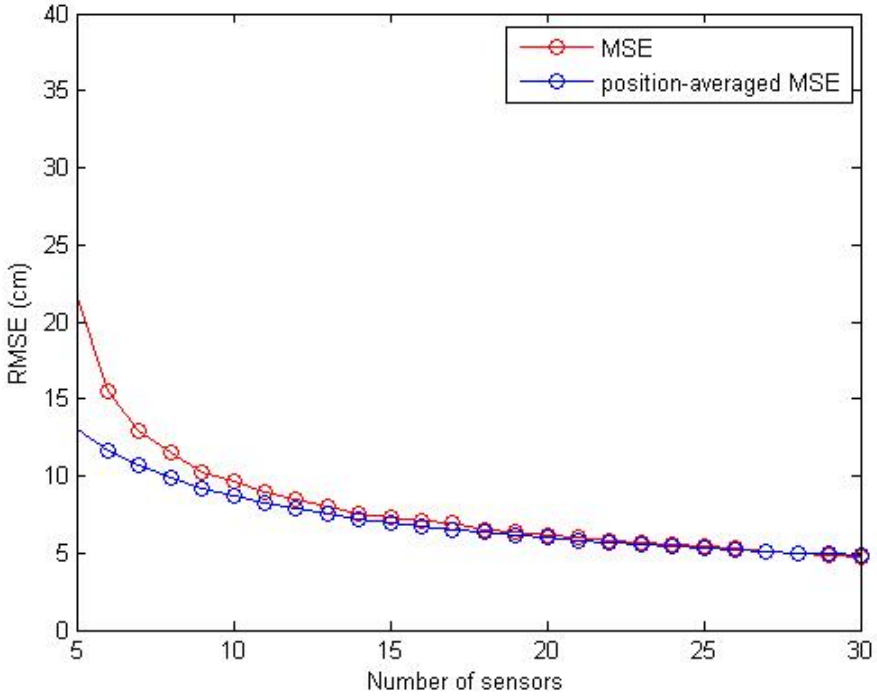

Figure 5.7 Closed-form MSE v.s. asymptotic MSE

From Figure 5.7, we can understand that the line of MSE and asymptotic MSE will asymptotically close to each other. It represent that the assumptions in Section 3.1 might hold when there are a large amount distributed sensors. To sum up, the closed-form MSE can be replace by a simpler closed-form shown in (5.4) asymptotically.

In Figures 5.6 and 5.7, the result of red line can be further improved by weighed LS solution which is derived in (3.14). In Figure 5.8, we can see the performance upgrade by WLS.

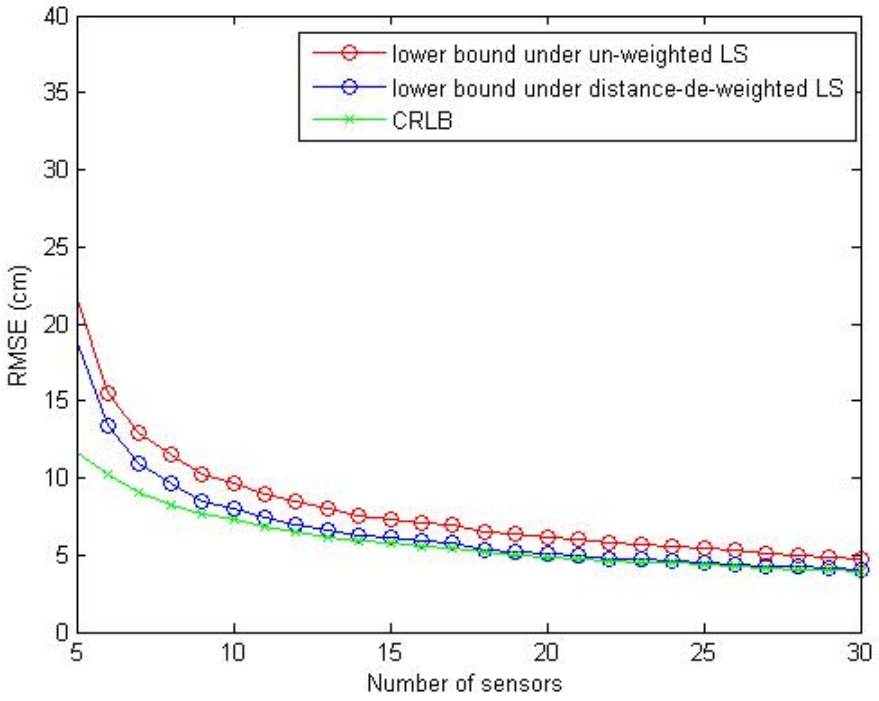

Figure 5.8 Performance improvement by Weighted LS

From Figure 5.8, we can understand that the red line is further improved to be the blue line. The amount of enhancement in performance is about 2cm (0.2σ). And from Figure 5.8 and (3.17), the hyperbolic positioning algorithm lower bound will approach to CRLB.

5.3 Asymptotic MSE of TS-approximated LS Solution

In this section, we show the simulation result of TS-approximated LS solution. As the derivation in Section 3.2, the simulated TS-approximated LS solution is bounded by (3.31) and (3.32). We can see Figure 5.9 shown below:

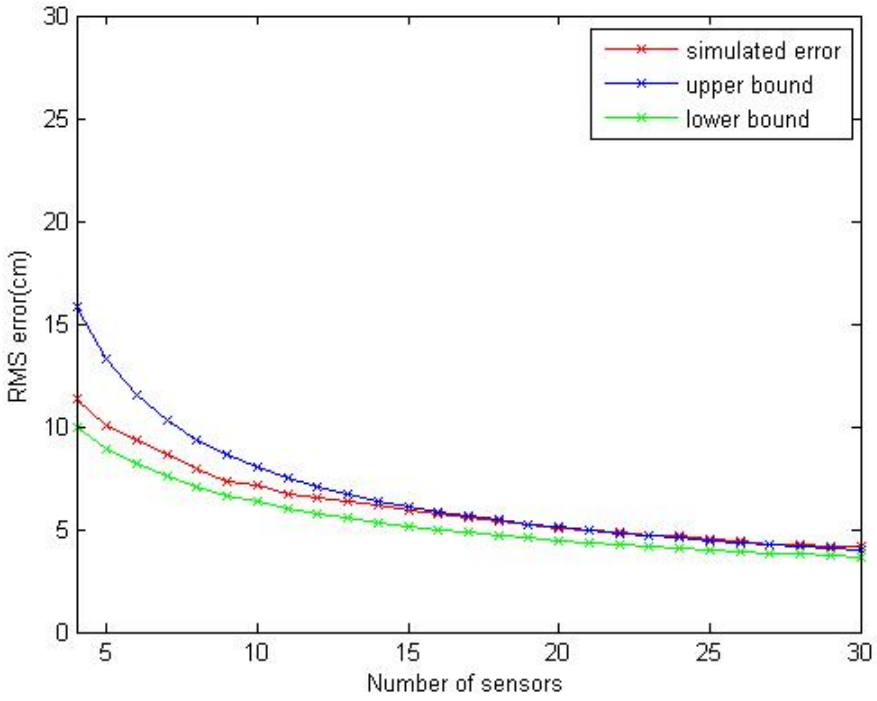

Figure 5.9 Lower bound and upper bound of TS-approximated localization errors-1

The red line is a simulated line using TS-approximated LS solution with modeling error. The modeling error is comes from the initial guess which is obtained from hyperbolic positioning algorithm. From Figure 5.9 we can understand that the simulated RMSE is actually bounded by blue line and green line. Also, the three lines will close to each other asymptotically as mention in Section 3.3. Besides, if the number of sensors is fixed (N=10), we can see the variation of performance with the variation of range error in Figure 5.10. The result is similar to Figure 5.9.

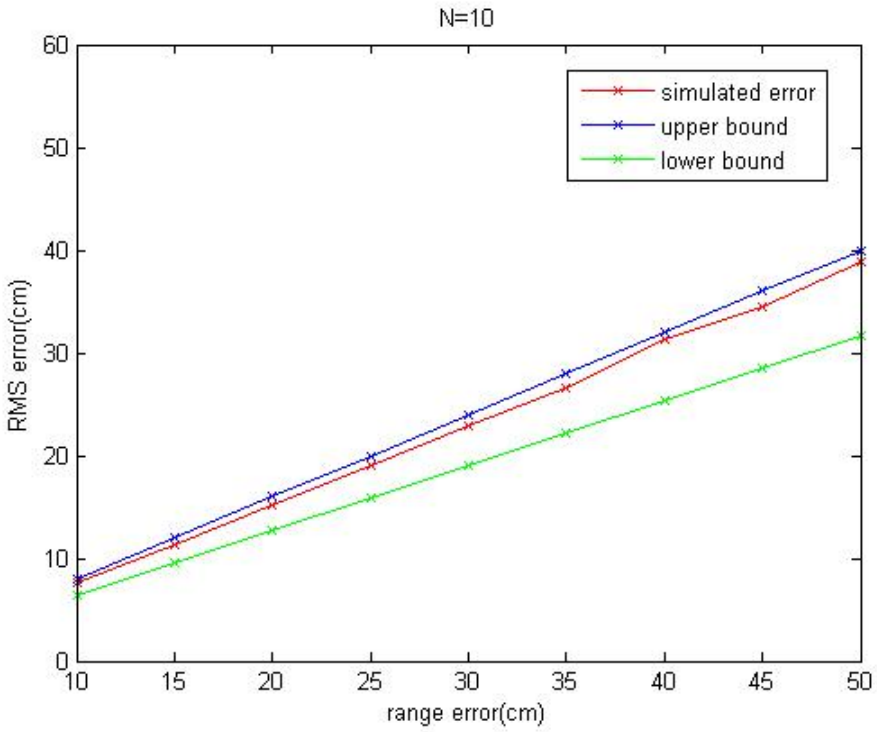

Figure 5.10 Lower bound and upper bound of TS-approximated localization errors-2

To sum up, we show the comparison of the linearization methods introduced in

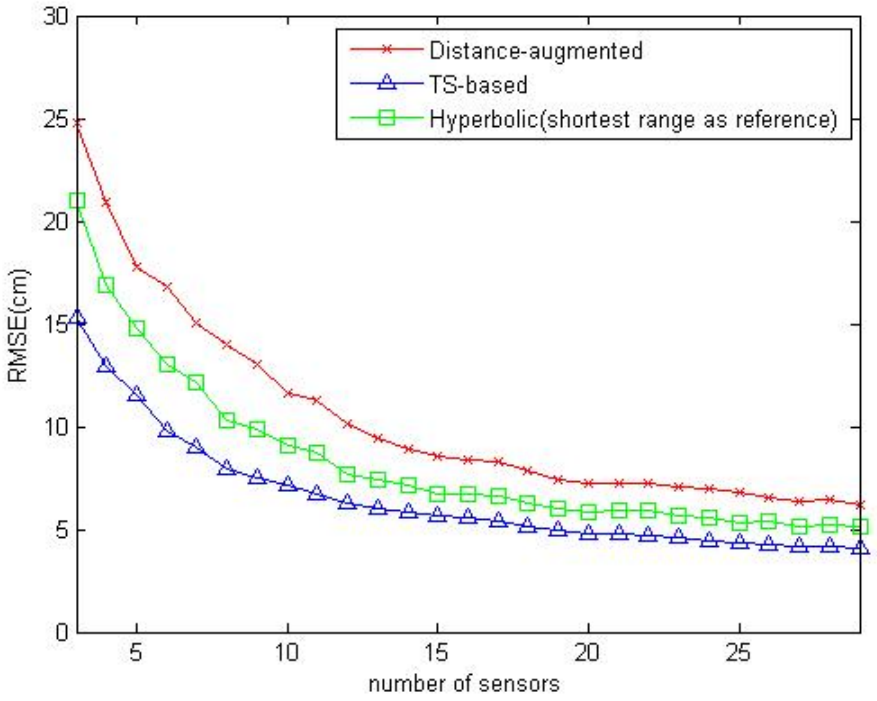

Figure 5.11 Comparison of 3 linearization methods

Section 2.5. Figure 5.11 shows the simulation result, and we can understand that TS-approximated localization outperforms the others. The simulation result also verifies the theoretical analysis which has been discussed in Chapter 3.

5.4 Coverage Analysis of TS-approximated Localization

From (4.2), the MSE of TS-approximated LS solution can be written as

$$f(\gamma) = \sigma^2 \times \frac{1}{(1-\gamma)} = \sigma^2 \times \frac{1}{(1-b^2-\delta^2)} \qquad (5.5)$$

Where both b and δ are position-dependent parameters. Once we know the value of b and δ, (5.5) can be calculated easily. Figure 5.13 shows the value of ε^2 at different position in a $6m \times 6m$ room and $\sigma = 10cm$. The four sensors are located at four corners respectively.

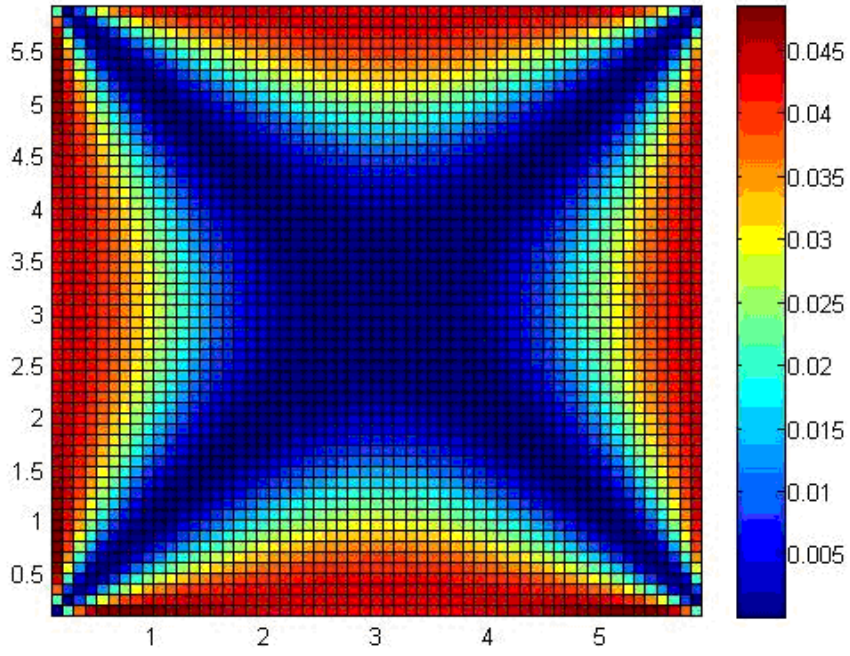

Figure 5.12 Value of ε^2 at different position

In Figure 5.12, we can understand that the value of ε^2 can almost be neglected because it is much smaller than 1. This result satisfies the mathematical derivation in

(4.8). Similarly, the value of δ^2 is shown in Figure 5.13 as following.

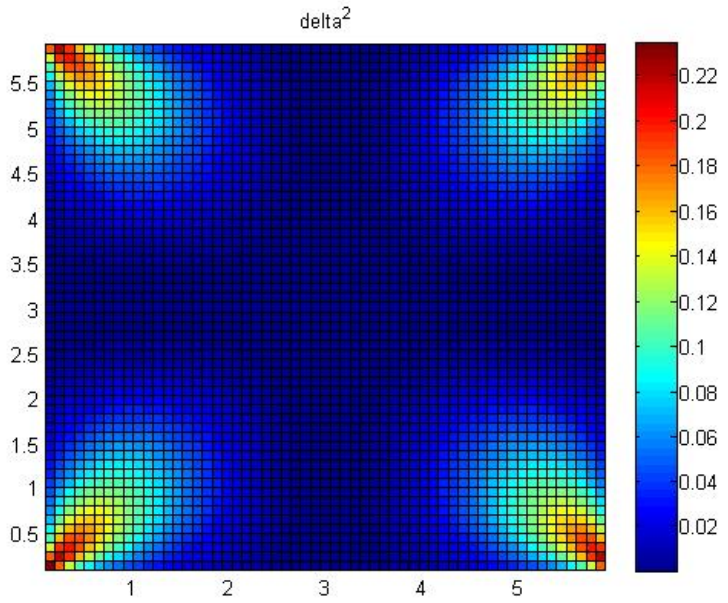

Figure 5.13 Value of δ^2 at different position

In Figure 5.13, we can understand that the value of δ^2 almost can reveal the localization error at different locations. When the mobile is closed to the sensor at corner, the value of δ^2 in (5.5) can't be neglected. In other words, the localization accuracy is somehow dominated by δ^2. Figure 5.14 shows the localization error for TS-approximated LS solution. We can understand that (5.5) and δ^2 have similar trend.

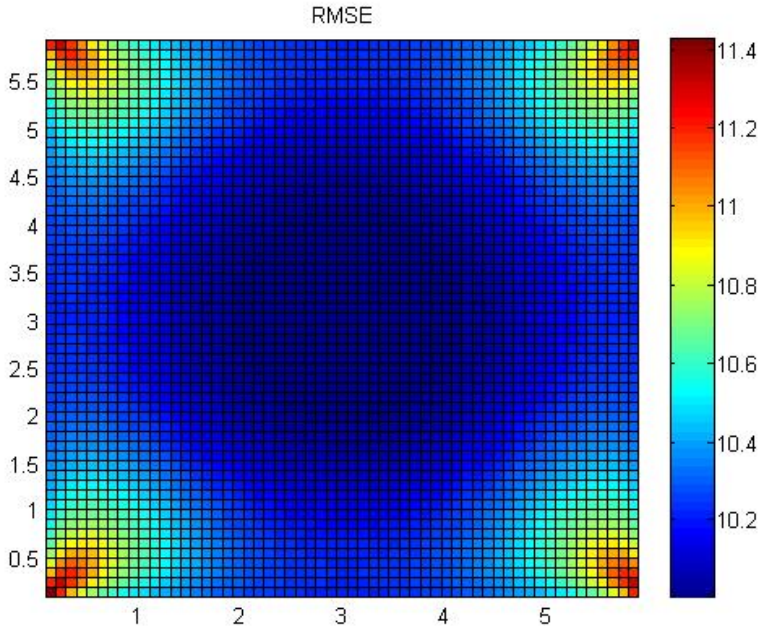

Figure 5.14 Localization error at different positions

5.5 Simulations of NLOS Mitigation

In this section, we will show the simulations to verify the algorithms proposed in Section 4.2. We assume the mobile locates at the center of a $30m \times 30m$ room. $\sigma = 0.4m$ for range error and $\sigma_L = 3m$ for NLOS bias error. Equivalently, the mean value and standard deviation for NLOS bias is 3.76 m and 1.97 m respectively. There are 8 sensors uniform distributed on the side of the room. We vary the number of NLOS sensors (denoted as m_L) and observe the performance between the four NLOS mitigation algorithm shown in Figure 5.15.

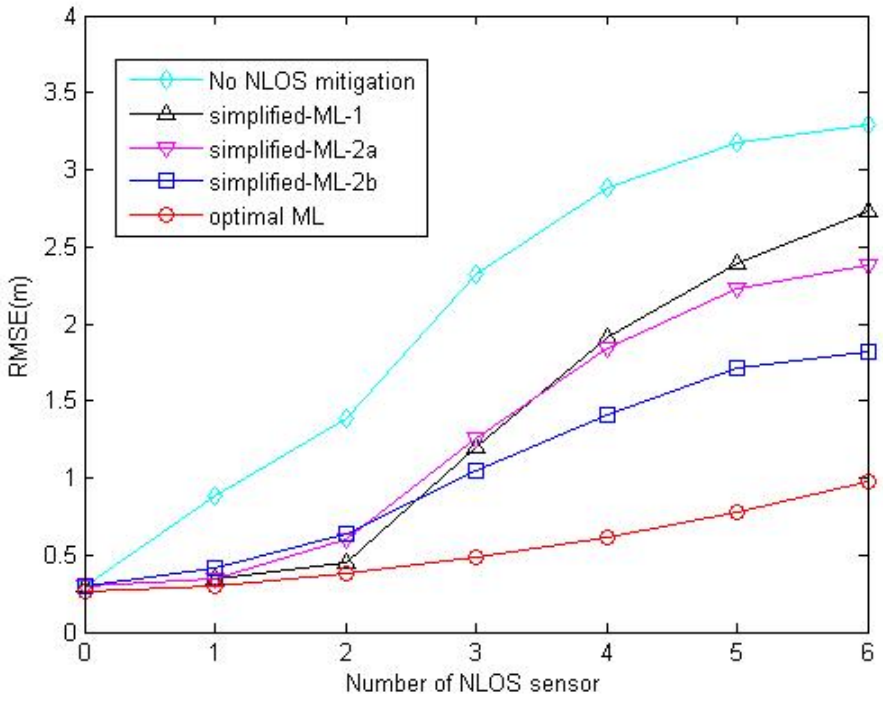

Figure 5.15 RMSE with different numbers of NLOS sensors.

From Figure 5.15, there are some observations. When $m_L < 3$, the two algorithms (simplified ML-2a, simplified ML-2b) we proposed are slightly worse than the algorithm proposed in [29] (simplified ML-1). But when $m_L \geq 4$, the proposed algorithms outperforms simplified ML-1. We infer that when there are a large amount of NLOS sensors, the NLOS bias would occur more likely around the true mean value of NLOS bias. So when $m_L \geq 4$, the effect of smoothing of least-squares will be more efficient. In Figure 5.16 and 5.17, we compare the CDF (Cumulative Density Function) when there are 2 and 5 NLOS sensors respectively.

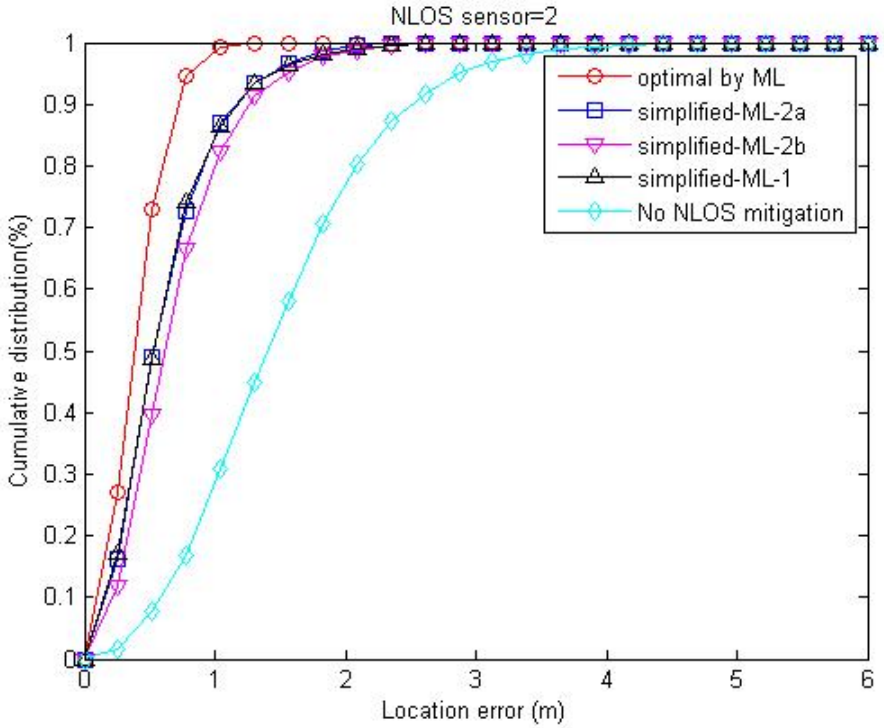

Figure 5.16 CDF comparisons with 2 NLOS sensors

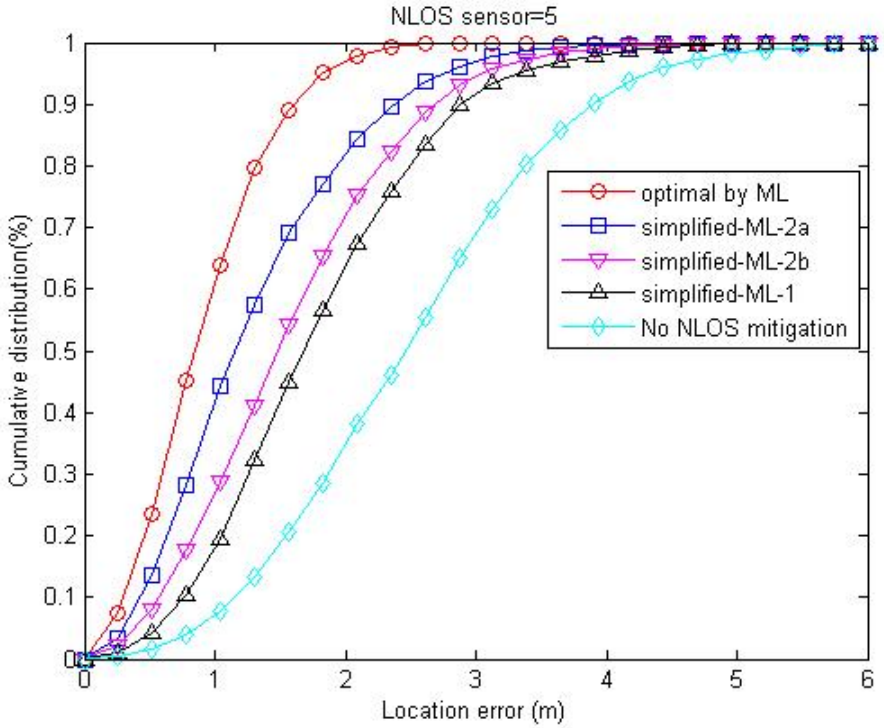

Figure 5.17 CDF comparisons with 5 NLOS sensors

In Figure 5.16, we can understand that the performances are comparable for the three algorithms (simplified ML-1, simplified ML-2a, simplified ML-2b) when there are 2 NLOS sensors. While if there are 5 NLOS sensors, the proposed two algorithms outperform simplified ML-1 obviously which verify our inference.

5.6 Simulation of Adaptive Localization

5.6.1 Simplified Kalman Filter and Conventional Kalman Filter

In Section 4.3 we proposed an adaptive location update by simplified Kalman filter. In this section, we compared the conventional Kalman with the simplified one. First, we set a trajectory for the mobile as Figure 5.18. The range error $\sigma = 10cm$ (high SNR). A point in Figures 5.18 and 5.19 is average by 100 position estimation. We can see the comparison in the Figures 5.18 and 5.19.

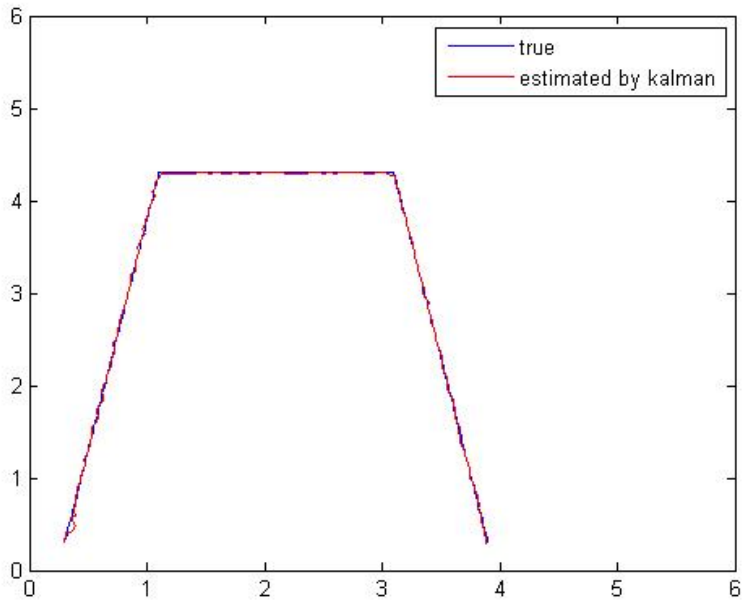

Figure 5.18 Conventional Kalman filter

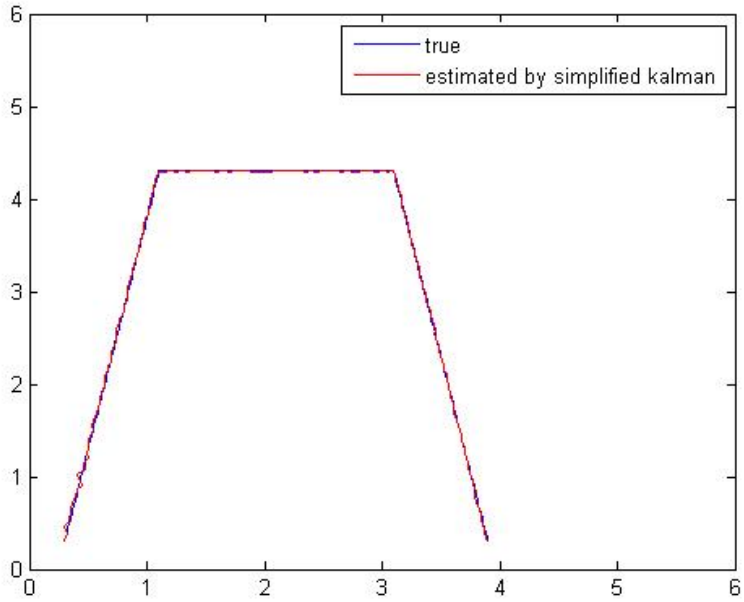

Figure 5.19 Simplified Kalman filter

From Figures 5.18 and 5.19, we can't recognize which method is the better one. However, the RMSE for conventional Kalman filter and simplified one is 1.23cm and 1.26 cm respectively. We can conclude that in high SNR environment, the two algorithms have comparable performance. In other words, we can save a portion of computational cost by using the proposed simplified Kalman filter. When the range error rises, we can see the comparison between the two algorithms in Figure 5.20.

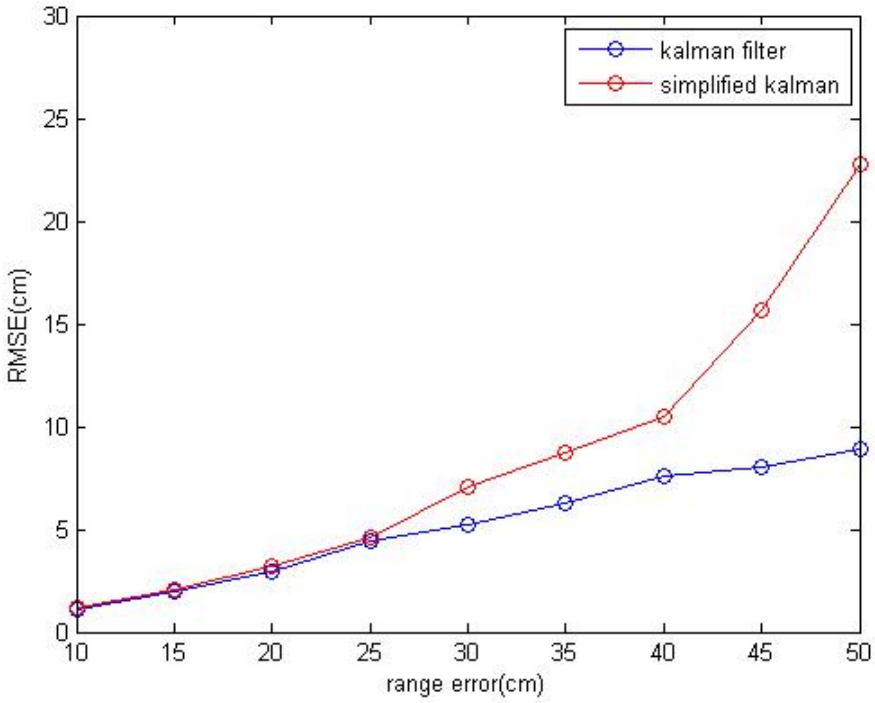

Figure 5.20 Adaptive localization performance v.s. range error

In Figure 5.20 we can understand that when the range error raises the difference between the two lines becomes larger and larger. In other words, conventional Kalman filter highly outperforms the simplified one. The main factor is the computation of Kalman gain. In Figure 4.8, when the range error rises, the assumption will degrade the accuracy of the calculation of Kalman gain. To sum up, adaptive localization using simplified Kalman gain saves amount of computational complexity in the cost of performance degradation.

5.6.2 Adaptive Localization with NLOS Bias Error

We also present our simulation on the adaptive localization with NLOS bias error. For simplicity, we assume a mobile is moving straightly from a corner to another corner as shown in Figure 5.21. NLOS error is randomly arranged in the route with random period. The NLOS bias error is modeled as Rayleigh distribution with mean 3.76m, standard deviation 1.97. And the range error is modeled as normal distribution with

$\sigma = 20cm$. We can see the simulation result as following Figure:

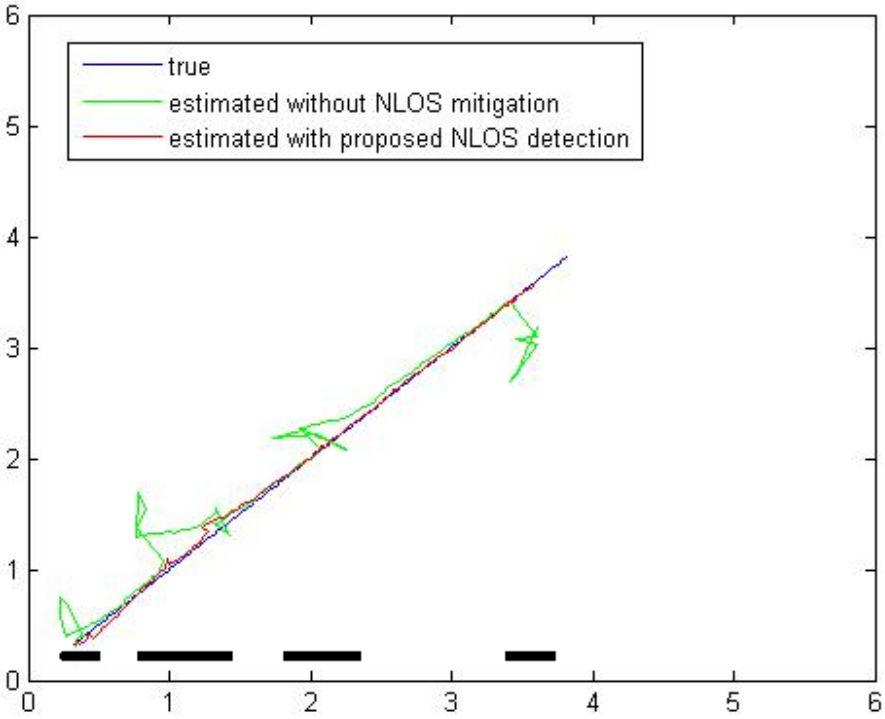

Figure 5.21 Adaptive localization in NLOS environment

The tracking line has been smoothed. The thick black line represents that the occurrence of NLOS effect. Without NLOS detection and mitigation, the tracking performance is shown as the green line which is poor while NLOS occurred. The red line is the tracking result by proposed NLOS detection scheme. We can understand that while the NLOS occurred, it can be detected by (4.33), and the tracking performance will still be not influenced by NLOS effect.

Chapter 6
Conclusions and Future Works

In this thesis, we improve the ranging accuracy by a scheme of a hybrid TOA and RSS. The improvement in ranging will enhance the accuracy of localization. And we have investigated the accuracy of linear least-squares solution for sensor network localization in LOS environment. And the asymptotic MSE for different least-squares techniques were derived. With the derivation in Chapter 3, we can interfere that the theoretical error of TS-approximated LS solution and lower bound of hyperbolic positioning algorithm achieves CRLB asymptotically. On the other hand, the asymptotic MSE is inversely proportional to the number of sensors from the derivation of this thesis.

From simulation results, the proposed NLOS mitigation algorithm with simplified ML outperforms the method proposed in [29] obviously. But there is still a gap between proposed simplified ML and exact ML solution. And if the NLOS has not been identified, the problem will be more challenging. Besides, we have shown the comparisons of proposed adaptive localization scheme and conventional one. In high SNR environment, they have comparable localization performance. But proposed adaptive localization using simplified Kalman Filter has lower computation cost. While in low SNR environment, the modified of proposed method to enhance performance is an issue which is deserve to discuss in the future.

Bibliography

[1] S .Srirangarajan, A. Tewfik; Z-Q. Luo, “Distributed sensor network localization using SOCP relaxation,” *IEEE Transactions on Wireless Communications* Volume 7, Part 1, pp. 4886 – 4895, Dec. 2008.

[2] P. Biswas, T-C Liang, K-C Toh, Y. Ye, and T-C Wang, “Semi-definite programming approaches for sensor network localization with noisy distance measurements,” *IEEE Transactions on Automation Science and Engineering* Volume 3, pp. 360 – 371, Oct. 2006.

[3] K-C. Ho, and Y. Le, “On the use of a calibration emitter for source localization in the presence of sensor position uncertainty,” *IEEE Transactions on Signal Processing* Volume 56, pp. 5758 – 5772, Dec. 2008

[4] N.A. Alsindi, B. Alavi, and K. Pahlavan, “Measurement and modeling of ultrawideband TOA-based ranging in indoor multipath environments,” *IEEE Transactions on Vehicular Technology* Volume 58, pp. 1046 – 1058, March 2009.

[5] D. Dardari, A. Conti, U. Ferner, A. Giorgetti, and M.Z. Win, “Ranging with ultrawide bandwidth signals in multipath environments,” *Proceedings of the IEEE* Volume 97, pp. 404 – 426, Feb. 2009.

[6] K.C. Ho, X.N. Lu, and L. Kovavisaruch, “Source localization using TDOA and FDOA measurements in the presence of receiver location errors: analysis and solution,“ *IEEE Transactions on Signal Processing* Volume 55, pp. 684 – 696, Feb. 2007

[7] A.N. Bishop, B. Fidan, B.D.O. Anderson, K. Dogancay; and P.N. Pathirana; “Optimal range-difference-based localization considering geometrical constraints ,” *IEEE Journal of Oceanic Engineering,* Vol. 33, pp. 289 – 301, July 2008.

[8] M. Souden, S. Affes, and J. Benesty, “A two-stage approach to estimate the angles of arrival and the angular spreads of locally scattered sources,”

IEEE Transactions on Signal Processing, Volume 56, pp. 1968 – 1983,May 2008.
[9] K.C. Ho, L.M.Vicente, "Sensor allocation for source localization with decoupled range and bearing estimation," *IEEE Transactions on Signal Processing*, Volume 56, pp 5773 – 5789, Dec. 2008.

[10] X. Li, "collaborative localization with received-signal strength in wireless sensor networks," IEEE Transactions on Vehicular Technology, Volume 56, pp. 3807 – 3817, Nov. 2007.

[11] H. Ren, and M. Meng, "Power adaptive localization algorithm for wireless sensor networks using particle filter," *IEEE Transactions on Vehicular Technology*, Volume 58, pp. 2498 – 2508, Jun 2009

[12] A. Broumandan, T. Lin, J. Nielsen, and G. Lachapelle, "Practical results of hybrid AOA/TDOA geo-location estimation in CDMA wireless networks," *2008. VTC 2008-Fall. IEEE 68th Vehicular Technology Conference*, pp. 1 – 5, Sep. 2008

[13] V. Vivekanandan, and V.W.S. Wong, "Concentric anchor beacon localization algorithm for wireless sensor networks," *IEEE Transactions on Vehicular Technology*, Volume 56, pp. 2733 – 2744, Sept. 2007.

[14] H. Wymeersch, J. Lien, and M.Z. Win, "Cooperative localization in wireless networks," *Proceedings of the IEEE* Volume 97, pp. 427 – 450, Feb. 2009.

[15]B-C Liu, K-H Lin, and J-C Wu, "Analysis of hyperbolic and circular positioning algorithms using stationary signal-strength-difference measurements in wireless communications," *IEEE Transactions on Vehicular Technology*, Volume 55, pp. 499 – 509, March 2006

[16] W. Wang, V. Srinivasan, B. Wang, and K-C Chua, "Coverage for target localization in wireless sensor networks," *IEEE Transactions on Wireless Communications*, Volume 7, pp. 667 – 676, Feb. 2008.

[17] I. Guvenc, C-C Chong, and F. Watanabe, "Analysis of a linear least-squares localization technique in LOS and NLOS environments," *Vehicular Technology Conference, 2007. VTC2007-Spring. IEEE 65th*, pp. 1886 – 1890, Apr. 2007.

[18] J.J. Caffery, ” A new approach to the geometry of TOA location,“ *IEEE VTS-Fall VTC 2000. 52nd Vehicular Technology Conference* Volume 4, pp. 1943 – 1949, Sept. 2000.

[19] D. Dardari, A. Conti, U. Ferner, A. Giorgetti, and M.Z. Win, “Ranging with ultrawide bandwidth signals in multipath environments,” *Proceedings of the IEEE* Vol. 97, pp. 404 – 426, Feb. 2009.

[20] D. Jourdan, D. Dardari, M. Win, “Position error bound for UWB localization in dense cluttered environments,” *IEEE Transactions on Aerospace and Electronic Systems*, Vol. 44, pp. 613 – 628, Apr. 2008.

[21] U. Sarac, F.K. Harmanci, T. Akgul, “Experimental analysis of detection and localization of multiple emitters in multipath environments,” *IEEE Antennas and Propagation Magazine*, Vol. 50, pp. 61–70, Oct. 2008.

[22] H-S Sheng and A.M. Haimovich, “Impact of channel estimation on ultra-wideband system design,” *IEEE Journal of Selected Topics in Signal Processing*, Volume 1, pp. 498 – 507, Oct. 2007.

[23] Y. Kim, B.F. Womack, “Performance evaluation of UWB systems exploiting orthonormal pulses,” *IEEE Transactions on Communications*, Volume 55, pp.929 – 935, May 2007.

[24] J. Scheuing and B. Yang, “Disambiguation of TDOA Estimates in multi-path multi-source environments (DATEMM),” *IEEE International Conference on ICASSP 2006 Proceedings*, Volume 4, pp. 4, May 2006.

[25] Y. Wang, W. Qun, B. Danping, and J. Jin, “Acoustic localization in multi-path aware environments,” *International Conference on ICCCAS 2007*, pp. 667 – 670, July 2007.

[26] I. Guvenc, C-C Chong, and F. Watanabe, “NLOS identification and mitigation for UWB localization systems,” *Wireless Communications and Networking Conference*, 2007, pp. 1571 – 1576, March 2007.

[27] W. Wang, J-Y Xiong, and Z-L Zhu, “A new NLOS error mitigation algorithm in location estimation,” *IEEE Transactions on Vehicular Technology,* Volume 54, pp. 2048 – 2053, Nov. 2005.

[28] Seow, C. Kiat, Tan, and S. Yim, “Non-line-of-sight localization in multipath environments,” *IEEE Transactions on Mobile Computing*, Volume 7, pp. 647 - 660, May 2008.

[29] K. Yu, and Y.J. Guo, “NLOS error mitigation for mobile location estimation in wireless networks,” *VTC2007-Spring. IEEE 65th*, pp. 1071 – 1075, April 2007.

[30] J. Yi, and M.R. Azimi-Sadjadi, “A robust source localization algorithm applied to acoustic sensor network,” *IEEE International Conference on ICASSP 2007*, Volume 3, pp. III-1233 - III-1236, April 2007.

[31] Z. Yi, and K. Chakrabarty, “Distributed mobility management for target tracking in mobile sensor networks,” *IEEE Transactions on Mobile Computing*, Volume 6, pp. 872 – 887, Aug. 2007.

[32] S. Aeron, V. Saligrama, and D.A. Castaon, “Efficient sensor management policies for distributed target tracking in multihop sensor networks,” *IEEE Transactions on Signal Processing*, Volume 56, pp. 2562 – 2574, June 2008.

[33] S. Liang, D. Hatzinakos, “A cross-layer architecture of wireless sensor networks for target tracking,” *IEEE/ACM Transactions on Networking*, Volume 15, pp. 145 – 158, Feb. 2007.

[34] G. Reina, A. Vargas, K. Nagatani, and K. Yoshida, “Adaptive Kalman Filtering for GPS-based mobile robot localization,“ *IEEE International Workshop on Safety, Security and Rescue Robotics 2007*, pp. 1 – 6, Sept. 2007.

[35] R. Zhan and J. Wan, “Iterated unscented Kalman Filter for passive target tracking,” *IEEE Transactions on Aerospace and Electronic System*s, Volume 43, pp. 1155 – 1163, July 2007.

[36] M. Ghaddar, L. Talbi, T.A. Denidni, and A. Sebak, “A conducting cylinder for modeling human body presence in indoor propagation channel,” *IEEE Transactions on Antennas and Propagation*, Volume 55, pp. 3099 – 3103, Nov. 2007.

[37] J-Y Lee and R.A. Scholtz, “Ranging in a dense multipath environment using an UWB radio link,” *IEEE Journal on Selected Areas in Communications*, Volume 20, pp. 1677 – 1683, Dec. 2002.

[38] M. Rydstrom, L. Reggiani, E.G. Strom, and A. Svensson, “Suboptimal soft range estimators with applications in UWB sensornetworks,” *IEEE Transactions on Signal Processing*, Volume 56, pp. 4856 – 4866, Oct. 2008.

[39] A. Beck, P. Stoica, and J. Li, “Exact and approximate solutions of source localization problems,” *IEEE Transactions on Signal Processing*, Volume 56, pp. 1770 – 1778, May 2008.

[40] Y-T Chan, Y-C Hang, and P-C Ching, “Exact and approximate maximum likelihood localization algorithms,” *IEEE Transactions on Vehicular Technology*, Volume 55, pp. 10 – 16, Jan. 2006.

[41] Laurendeau, C.; Barbeau, M., “Hyperbolic location estimation of malicious nodes in mobile WiFi/802.11 networks,” *33rd IEEE Conference on Local Computer Networks*, pp. 600 – 607, Oct. 2008.

[42] W. H. Foy, “Position-location solutions by Taylor-series estimation,” IEEE Trans. Aerospace and Electronic Systems, Volume. 12, pp. 187—194, Mar. 1976.

[43] P. Tarrio, A.M. Bernardos, J.A. Besada, and J.R. Casar, “A new positioning technique for RSS-Based localization based on a weighted least squares estimator,” *IEEE International Symposium on Wireless Communication Systems*, pp. 633 – 637, Oct. 2008.

[44] H. Farrokhi, and R.J. Palmer, “The designing of an indoor acoustic ranging system using the audible spread spectrum LFM (chirp) signal,” *Canadian Conference on Electrical and Computer Engineering*, pp. 2131 - 2134, May 2005.